The Plant Cell, Vol. 20: 901–919, April 2008, www.plantcell.org 

# *REBELOTE*, *SQUINT*, and *ULTRAPETALA1* Function Redundantly in the Temporal Regulation of Floral Meristem Termination in *Arabidopsis thaliana* [W]

**Nathanaël Prunet,[a,1] Patrice Morel,[a,1] Anne-Marie Thierry,[a] Yuval Eshed,[b] John L. Bowman,[c] Ioan Negrutiu,[a] and Christophe Trehin[a,2]**

[a] Laboratoire de Reproduction et Développement des Plantes, Université de Lyon, Centre National de la Recherche Scientifique, Institut National de la Recherche Agronomique/Ecole Normale Supérieure, F-69347 Lyon cedex 07, France
[b] Department of Plant Sciences, Weizman Institute of Science, Rehovot, 76100, Israel
[c] School of Biological Sciences, Monash University, Melbourne, Vic 3800, Australia

**In *Arabidopsis thaliana*, flowers are determinate, showing a fixed number of whorls. Here, we report on three independent genes, a novel gene *REBELOTE* (*RBL*; protein of unknown function), *SQUINT* (*SQN*; a cyclophilin), and *ULTRAPETALA1* (*ULT1*; a putative transcription factor) that redundantly influence floral meristem (FM) termination. Their mutations, combined with each other or with *crabs claw*, the genetic background in which they were isolated, trigger a strong FM indeterminacy with reiterations of extra floral whorls in the center of the flower. The range of phenotypes suggests that, in *Arabidopsis*, FM termination is initiated from stages 3 to 4 onwards and needs to be maintained through stage 6 and beyond, and that *RBL*, *SQN*, and *ULT1* are required for this continuous regulation. We show that mutant phenotypes result from a decrease of *AGAMOUS* (*AG*) expression in an inner 4th whorl subdomain. However, the defect of AG activity alone does not explain all reported phenotypes, and our genetic data suggest that *RBL*, *SQN*, and, to a lesser extent, *ULT1* also influence SUPERMAN activity. Finally, from all the molecular and genetic data presented, we argue that these genes contribute to the more stable and uniform development of flowers, termed floral developmental homeostasis.**

## INTRODUCTION

Flowers are the reproductive structures that characterize angiosperms. They contain the male and female reproductive organs (stamens and carpels), often surrounded by outer sterile structures (sepals and petals). Floral organ identity is controlled by a set of genes that apparently act according to the quartet model (Ferrario et al., 2004; Jack, 2004; Angenent et al., 2005). In *Arabidopsis thaliana*, this model postulates that, together with the E class genes *SEPALLATA1* (*SEP1*) to *SEP4*, the A class genes *APETALA1* (*AP1*) and *AP2* control sepal and petal identities, the B class genes *AP3* and *PISTILLATA* (*PI*) control petal and stamen identities, and the C class gene *AGAMOUS* (*AG*) controls stamen and carpel identities.

In the eudicot plant *Arabidopsis*, the flower is determinate: floral organs are in whorls, with a fixed number of whorls and parts per whorl, and internodes between whorls that do not elongate. By contrast, in many angiosperms outside the core eudicots, flowers are somewhat indeterminate and display morphological variations, such as a variable number of whorls and parts per whorl, an extensive elongation of the floral axis, or a spiral phyllotaxy. It is thought that variations of floral axis determinacy and compression (with a decrease of floral organ number) are two major evolutionary innovations that produced compact angiosperm flowers (Baum and Hileman, 2006) and that these two evolutionary innovations are manifestations of an increased floral developmental homeostasis (i.e., the tendency to produce a fixed number of structures in stereotypical positions; Frohlich, 2006). Some angiosperms would have retained the ancestral condition of weak developmental homeostasis, whereas core eudicots, including *Arabidopsis*, would have evolved strong floral homeostasis. However, underlying cellular and developmental mechanisms remain elusive and, except for AG and WUSCHEL (WUS) (see below), little is known about factors involved in these processes. A better understanding of these processes could result from the isolation of new regulatory factors from model plants.

Flowers develop from flower meristems (FMs), which in turn are produced at the flank of inflorescence shoot apical meristems (iSAMs; Blazquez et al., 2006). Therefore, the FM initially inherits the potential of indeterminacy from the iSAM, manifested in the maintenance of a stem cell population located in the center of the meristem. This maintenance is based on a feedback loop involving *WUS* and *CLAVATA1* (*CLV1*), *CLV2*, and *CLV3* genes, the mechanistic nature of which is unknown (Carles and Fletcher, 2003; Doerner, 2006). *WUS*, expressed in the deeper layers of meristems (Mayer et al., 1998), maintains *CLV3* expression in stem cells, located in the upper two layers of the central zone. In

[1] These authors contributed equally to this work.
[2] Address correspondence to ctrehin@ens-lyon.fr.
The author responsible for distribution of materials integral to the findings presented in this article in accordance with the policy described in the Instructions for Authors (www.plantcell.org) is: Christophe Trehin (ctrehin@ens-lyon.fr).
[W] Online version contains Web-only data.
www.plantcell.org/cgi/doi/10.1105/tpc.107.053306

turn, *CLV* genes inhibit *WUS* and thus regulate the size of the stem cell population (Fletcher et al., 1999; Brand et al., 2000; Schoof et al., 2000). FMs become determinate after the initiation of carpel primordia, but determinacy is likely initiated earlier since *WUS* expression starts declining from stage 3, prior to the initiation of the carpels (Mayer et al., 1998; stages are all defined according to Smyth et al., 1990). AG is of particular importance in specifying FM determinacy since it is part of a second feedback loop, set up in the FM, which is superimposed on the *CLV*/*WUS* feedback loop. This second feedback loop starts with the activation of *AG* expression by WUS together with LEAFY at stage 3 of floral development (Parcy et al., 1998; Busch et al., 1999; Lenhard et al., 2001; Lohmann et al., 2001). In turn, AG turns *WUS* expression off, likely indirectly (Sieburth et al., 1998), resulting in the arrest of stem cell maintenance in the center of the FM. Mutations in *AG* and *CLV* genes or ectopic expression of *WUS* beyond stage 6 are sufficient to induce floral meristem indeterminacy (Bowman et al., 1989; Clark et al., 1993; Shannon and Meeks-Wagner, 1993; Clark et al., 1995; Lenhard et al., 2001; Lohmann et al., 2001).

Interestingly, *CLV* and *AG* illustrate different levels of the control of FM size and determinacy. In a *clv* null allele, the FM is significantly enlarged. It produces more primary floral organs in all whorls than the wild-type plants and one or two additional whorls of carpels in the center of the flower, inside the primary carpels (Clark et al., 1993; Dievart et al., 2003). The increase of FM size results from an enlarged *WUS* expression domain and supernumerary whorls of carpels from delayed *WUS* extinction (Schoof et al., 2000). In *ag* mutants, the FM is not enlarged. Organ numbers per whorl are not increased, but a large number of extra whorls develop from the center of flower, resulting in a flower-within-a-flower phenotype, or Russian doll (Bowman et al., 1989; Sieburth et al., 1995). Accordingly, *WUS* expression remains spatially restricted but is not switched off (Lenhard et al., 2001; Lohmann et al., 2001). The temporal regulation of *WUS* extinction, which prevents the development of supernumerary whorls in the center of the FM, is here defined as FM termination and will be discussed in this article.

Other regulators also regulate FM termination. *ULTRAPETALA1* (*ULT1*) was shown to prevent the formation of extra primary floral organs and of supernumerary carpel whorls (Fletcher, 2001; Carles et al., 2005). Reported data suggest that *ULT1* operates in the *AG* pathway. *SUPERMAN* (*SUP*), whose mutations result in an increase of primary stamen and carpel numbers, depending on the allele (Schultz et al., 1991; Bowman et al., 1992; Gaiser et al., 1995), also affects FM termination. *AG* and *SUP* act synergistically since the double mutant consists of reiterations of petals produced by an indeterminate and fasciated FM (Schultz et al., 1991; Bowman et al., 1992), but the interconnections between *AG* and *SUP* functions remain an enigma (Sakai et al., 2000; Gomez-Mena et al., 2005; Sablowski, 2007). It is postulated that *SUP* controls FM termination by preventing B class gene expression in the 4th whorl. This is corroborated by the fact that, in *Arabidopsis* and *Antirrhinum majus*, B class mutants are overdeterminate and that flowers ectopically expressing B class genes are partially indeterminate (Hill and Lord, 1989; Sommer et al., 1990; Schultz et al., 1991; Bowman et al., 1992; Trobner et al., 1992; Krizek and Meyerowitz, 1996; Sakai et al., 2000). Recently, miR172-mediated regulation of *AP2* was also shown to be crucial for floral termination (Chen, 2004; Zhao et al., 2007). Ectopic expression of miR172-resistant *AP2* triggers FM indeterminacy with flowers producing an indeterminate number of either petals or stamens. In the transgenic lines producing supernumerary stamens, the B class gene *PI* is ectopically expressed in the center of the FM and *WUS* expression is prolonged (Zhao et al., 2007). The authors proposed that this miR172-dependant *AP2* regulatory pathway acts through both the *AG* and *CLV* pathways.

Examples reported above show that the manifestations of FM termination defects are diverse but can be distinguished as defects that take place before primary carpel development (corresponding to early events of FM termination; e.g., miR172-resistant *AP2* and *sup* phenotypes) or defects that take place after (corresponding to late events of FM termination; e.g., *ag* and some aspects of *clv* and *ult1* phenotypes). However, since these two types of indeterminacy have not been observed in the same mutant backgrounds, one can wonder whether they reflect a continuous regulation of FM termination.

*CRABS CLAW* (*CRC*) is the founding member of the YABBY gene family (Bowman and Smyth, 1999). Its expression is largely limited to carpels and nectaries (Bowman and Smyth, 1999). In *crc* loss-of-function mutants, carpels are shorter, unfused at their top (the so-called crabs claw phenotype; Alvarez and Smyth, 1999), and display polarity defects (Eshed et al., 1999), while nectaries fail to develop (Bowman and Smyth, 1999). However, the development of supernumerary whorls inside primary carpels observed in *crc-1 spatula-2* (*spt-2*) and *crc-1 ag-1*/+ double mutants suggested that *CRC* could also influence FM termination (Alvarez and Smyth, 1999). Based of this observation, we performed a modifier mutagenesis screen in the *crc-1* background (Bowman et al., 2001), which allowed us to isolate and analyze three independent factors that act redundantly with *CRC* and with each other in controlling FM termination. From double and triple mutant combinations, we were able to define two major categories of phenotypes. The first shows a recurrent reset of the FM with the production of extra floral organs inside the gynoecium, corresponding to defects in late events of FM termination, and the second displays a large increase in numbers of primary floral organ whorls, particularly stamens, corresponding to defects in early events of FM termination.

## RESULTS

### *crc-1* Modifiers Reveal a Range of Floral Indeterminacy Syndromes

T-DNA and ethyl methanesulfonate (EMS) mutagenesis experiments were performed in the *crc-1* background to screen for modifiers of the *crc* phenotype (Figure 1). The *crc-1* mutation limits style development and disrupts distal carpel fusion, (Figure 1B, left) but very rarely affects FM determinacy (Alvarez and Smyth, 1999). Upon screening several thousand M2 (EMS mutagenesis) and T2 (T-DNA mutagenesis) families, three independent mutants of similar phenotype were recovered. In a *crc* background, each triggers FM indeterminacy associated with reiterated whorls produced internal to the primary carpels (Figures 1B to 1H). A detailed analysis of the three double mutants

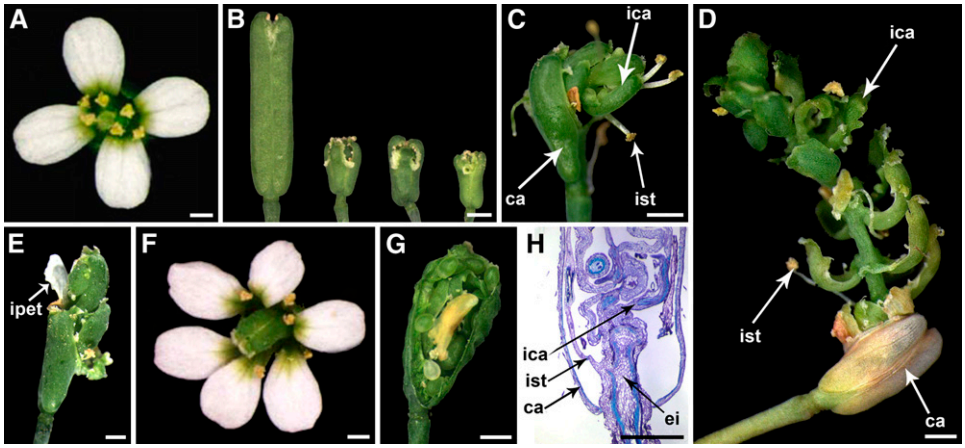


**Figure 1.** Phenotypes of the *crc-1 rbl-1*, *crc-1 sqn-4*, and *crc-1 ult1-4* Double Mutants.

**(A)** *crc-1* flower.
**(B)** From the left to the right, siliques from *crc-1*, *crc-1 rbl-1*, *crc-1 sqn-4*, and *crc-1 ult1-4* double mutants. Compared with *crc-1*, the double mutant siliques are shorter and enclose extra floral organs.
**(C)** to **(E)** Double mutant (*crc-1 rbl-1* in **[C]** and **[E]** and *crc-1 sqn-4* in **[D]**) siliques at various developmental stages. Reiterations of stamens (ist), carpels (ica), and sometimes petals (ipet, **[E]**) occur inside the primary carpels (ca). Such indeterminacy might produce a 5- to 15-mm floral axis bearing groups of stamens and carpels, with visible internodes, according to a whorled phyllotaxy **(D)**.
**(F)** *crc-1 ult1-4* flower with more petals.
**(G)** Example of a weak indeterminacy phenotype (observed in *crc-1 ult1*-4) where extra organs do not grow outside primary carpels. A carpel was removed to show internal structures.
**(H)** Close-up view of the base of a young *crc-1 rbl-1* double mutant silique (toluidine staining). The floral axis that bears extra stamens (ist) and carpels (ica) displays elongated internodes (ei) and grows from the bottom of the silique between the two carpels (ca); similar pictures were obtained with *crc-1 sqn-4* and *crc-1 ult1-4*.
Bars = 500 μm.

was then performed. The names of alleles, *rebelote-1* (*rbl-1*; ''once again'' in French), *squint-4* (*sqn-4*), and *ultrapetala1-4* (*ult1-4*), are based on the cloning of the genes, which is described below (Figure 2).

All three double mutants develop shorter gynoecia than *crc-1* (Figure 1B) and reiterate extra whorls of stamens, carpels, and occasionally petals in the center of the flower (Figures 1C to 1E and 1G). Such reiterations always preserve a wild-type whorl organization (i.e., stamens-carpels or petals-stamens-carpels). Nevertheless, differences exist between the three mutants. Phenotypic scoring (Table 1) shows that 100% of *crc-1 rbl-1* flowers are indeterminate, whereas 86% of *crc-1 sqn-4* flowers and 83% of *crc-1 ult1-4* flowers produce extra whorls. In addition, among the *crc-1 rbl-1* indeterminate flowers, 91% break through the gynoecium and grow outside the silique (Figures 1C and 1D). Such elongated axes are observed in ~25% of *crc-1 sqn-4* and more rarely in *crc-1 ult1-4* flowers. Strong indeterminacy phenotypes show new floral organs developing even while the rest of the plant is senescent (Figure 1D), indicating a permanent loss of determinacy. In cases of less-pronounced indeterminacy, the gynoecium morphology is usually similar to *crc-1*, except that there is a mild increase of carpel number (Table 1), with ectopic stamens and carpels developing inside the pistil (Figure 1G). Despite a slight variability from one experiment to another, the same tendency in the strength of the phenotype (*rbl-1* > *sqn-4* > *ult1-4*) is always observed between the mutations in combination with *crc-1*. Whatever the strength of the phenotype, internal organs produced inside the ovary greatly compromise fertility. In addition to the indeterminacy observed at the FM center, the *crc-1 ult1-4* double mutant develops additional sepals and petals on the two outermost whorls similar to *ult1* single mutants (Figure 1F, Table 1), whereas neither *crc-1 rbl-1* nor *crc-1 sqn-4* display such a phenotype.

Observations of gynoecium development show that the ectopic floral organs produced in double mutants arise at the base of and adaxial to the primary carpels (Figure 4). At floral stage 6, while carpel primordia appear tightly joined in wild-type flowers (Figure 4A), they are separated by a cell dome, similar to a meristem, in *crc-1 rbl-1*, *crc-1 sqn-4*, and *crc-1 ult1-4* double mutants (Figures 4B to 4D). During later flower development, the ectopic organs or structures stay firmly attached to an elongating axis at the base of the silique (Figure 1H).

In summary, in combination with *crc-1*, the three mutations make the FM indeterminate, with ectopic stamens and carpels developing from the very center of the FM, between primary carpels, and on an elongated axis. *RBL*, *SQN*, and *ULT1* therefore influence late events (stage 6 and beyond) of FM termination and are collectively essential for normal floral axis compression. The reiteration of stamens and petals implies a reactivation of B class genes after carpel formation.

### Cloning of *crc* Modifier Genes

The molecular identity of the two EMS-induced *crc* modifiers was determined via map-based cloning. The mutation in *RBL* was

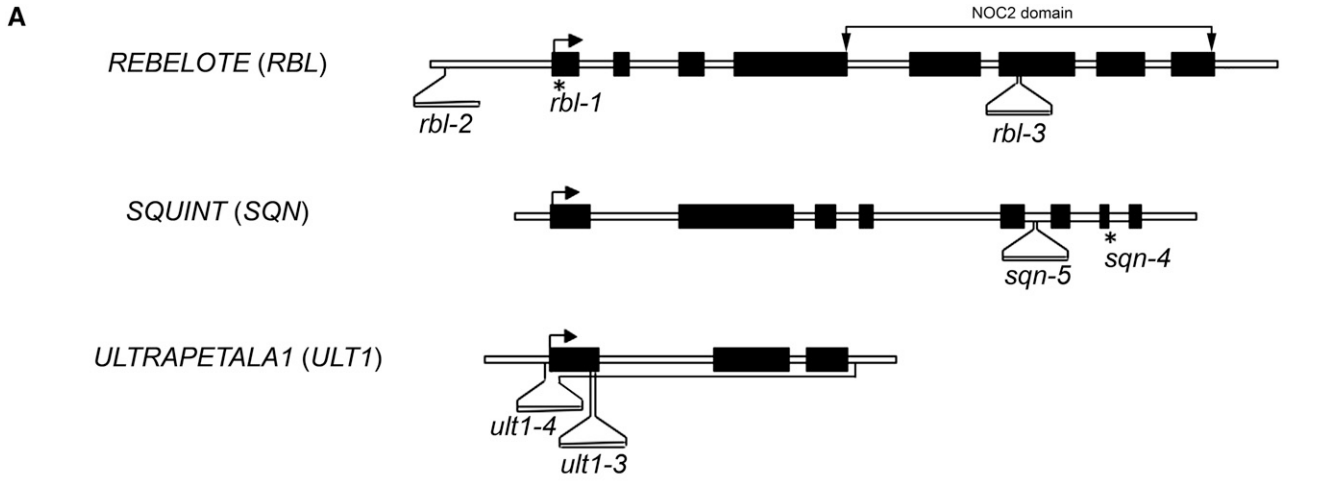


B

```
                RBL=At3G55510  (256) IKISVHLWVTG-EETISQQAFLILKDISMVFNSECFDSCLINMYKAFLHDCDIPKANSEQRP-ELRDSLVPLCSQDVQKSYTKASVSITQ
                      At2g18220  (292) IKVALHFWGTG-SGALPVVSLLFLRDLCIRLGSDCVDDCFKGMYKAYVLNCQFVNADKLKHISELGNCFIPLLGTDISAAYQHAFVFIRQ
          Chicken_NP_001026047  (281) LKQAIHLWSTG-EETVRVLSFLVLNKICRHRKEVYLSPLLKQMYIAFVKNSRFTSPNVLPMINEMQRTLTPMYALDTHTSYQHAFIYIRQ
            Cow_NP_001029498.1  (290) LKRMVVLWSTG-EETLRVLAFVVLIKVCRHKKDVFLSPVLKQMYITYVRNCKFTSPSTLPLINEMQRTLTPLLALDTGVAYQHAFLYIRQ
              Dog_XP_546728.2  (306) LKRMVVLWSTG-EETLRVLAFLVLVRVCRHKKEVFLSPILKQMYITYVRNCKFTSPSTLPFINEMQRTLIPLLALDTGIAYQHAFLYIRQ
          Fruitfly_NP_610095.1  (312) LKRLVVLWSTG-DETVRVLAFLCILKITRKQQATMLNHVLKAMYLAYVRNSKFVSPNTLPGINEMRRSLVPMFALDLNVSYQHVFLYIRQ
             Human_NP_056473.1  (295) LKRMVVVWSTG-EESLRVLAFLVLSRVCRHKKDTFLGPVLKQMYITYVRNCEFTSPGALPFISEMQWTLTPLLALEPGVAYQHAFLYIRQ
            Mouse_NP_067278.1  (299) LKRMVVLWSTG-EESLRVLAFLVLIRVCRHKKEAFLGPILKQMYIMYVRNCKFTSPSTLPLISEMQRTLTPMLALDPSVSYQHAFLYIRQ
           Rat_NP_001029069.1  (192) VKRMIVLWSTG-EESLRVLAFLVLIKVCRHKKESFLGPILKQMYIMYVRNCKFTSPSTLPLISEMQRTLTPLLALDPSVSYQHAFLYIRQ
            Yeast_NP_014849.1  (319) IKSIVGVWSPTRELETQIASFAFLINTTKEFKKSMLETTLKTTYSTFIKSCRKTNMRSMPLINFQKNSAAPLFGIDEVLGYQVGFEYIRQ
                    Consensus  (364) LKRMVVLWSTG EETLRVLAFLVLIKVCRHKKE FL PILKQMYI YVRNCKFTSP TLPLINFMQRTLTELLALD  VSYQHAFLYIRQ

                RBL=At3G55510  (344) LAKLLKMALATKNK--------EAVEKIHSGEYINCVDLWVNFISANVQDCD-------LQPLLYTIVQVINGVAQIIIGPRYLLLRVKC
                      At2g18220  (381) LAMILREALNTKTK--------EAFRKVYQWKFIHCLELWTGAVCAYSSQSE-------LRPVAYPLAQIITGVARLVPTARYTPLRLRC
          Chicken_NP_001026047  (370) LAIHLRSAMTIKKK--------ENFQSVYNWQYVHCLYFWCRVLSTIYPSEV-------MEPLIYPLTQVIIGCIKLVPTARFYPLRMHC
            Cow_NP_001029498.1  (379) LAIHLRNAMTTRRK--------ETYQSVYNWQFVHCLYLWCRALSTICPSEA-------LQPLIYPLSQVVIGCIKLVPTARFYPLRMHC
              Dog_XP_546728.2  (395) LAIHLRNAMTTRKK--------ETYQSVYNWQFVHCLYLWCRALSTVCPSEA-------LQPLIYPLSQVVIGCIKLVPTARFYPLRMHC
          Fruitfly_NP_610095.1  (401) LAIHLRNAVILKKK--------DSFQAVYNWQFINSLRLWADLLGASANKPQ-------LQPLIYPLVTIATGVIRLIPTAQYFPLRFHC
             Human_NP_056473.1  (384) LAIHLRNAMTTRKK--------ETYQSVYNWQYVHCLFLWCRVLSTAGPSEA-------LQPLVYPLAQVIIGCIKLIPTARFYPLRRMHC
            Mouse_NP_067278.1  (388) LAVHLRNAMTAGKK--------ETHQSVYNWQYVHCLYLWCRVLSTLGSSEI-------LQPLLYPLSQIIIGCIKLLPTARFYPLRRMHC
           Rat_NP_001029069.1  (281) LAVHLRNAMTTGKK--------ETYQSVYNWQYVHCLYLWCRVLSALGSSEV-------LQPLLYPLSQIIIGCIKLLPTARFYPLRRMHC
            Yeast_NP_014849.1  (409) LAIHLRNTMNATTKKSSKINSAEAYKIVYNWQFCHSLDFWSRVLSFACQPEKENGSESPLRQLIYPLVQVTLGVIRLIPTPQFFPLRFYL
                    Consensus  (454) LAIHLRNAMTTKKK         ETYQSVYNWQFVHCLYLWCRVLSTI   SE         LQPLIYPLSQVIIGCIKLIPTARFYPLRMHC

                RBL=At3G55510  (419) IHWLNHLSRTSGIFIPIASLVLDMLEYKTTNDGEKQ---EQKLEAVSTVKLPKNWLKSQNFQEQCIFSVIELLAVHFAQWSFHISSPDLA
                      At2g18220  (456) VRMLNRLAAATGTFIPVSMLLVDMLEMKELNRPPTG-GVGKGVDLRTLLKVSKPAVKTRAFQEACVYTVVEELVEHLSQWSCSVASFELS
          Chicken_NP_001026047  (445) IRALTLLSENTRTFIPVLPFILEVFQQVDFNKRPGR-MSAKPINFAVILKLSNANLQEKAYRDGLVDQLYDLILEYLHCQAHSIGSPELF
            Cow_NP_001029498.1  (454) VRALTLLSESTGTFIPVLPFILEIFQQVDFNRRPGR-ISSRPINFAVILKLSKVNLQEKAYRDGLVEQLYDLTLEYLHSQAHSIASPELV
              Dog_XP_546728.2  (470) VRALTLLSESTGTFIPVLPFILEVFQQVDFNRRPGR-MSSKPINFMVILKLSKVNLQEKAYRDGLVEQLYDLILEYLHSQAHSIASPELA
          Fruitfly_NP_610095.1  (476) LQTLISLAKETNTYVPVLPLIVEVLKSNTFNRKHSA-VSMKPVQFTCVLRLNKGQLAENGFRDEVIEQVCGLLLEYLAHESTSLASSDLV
             Human_NP_056473.1  (459) IRALTLLSGSSGAFIPVLPFILEMFQQVDFNRKPGR-MSSKPINFSVILKLSNVNLQEKAYRDGLVEQLYDLTLEYLHSQAHCIGSPELV
            Mouse_NP_067278.1  (463) VRALTLLSQTIGTFIPVLPFILEIFQQVDFNRRPGR-MSSKPINFSVILKLSSTNLQEKAYRDGLLEQLCDLTLEYLHSQAHSIASPELV
           Rat_NP_001029069.1  (356) VRALTLLSQTVGTFIPVLPFILEIFQQVDFNKRPGR-MSSKPINFSVILKLSSTNLQEKAYRDGLLEQLYDLIMEYLHGQAHSIASPELV
            Yeast_NP_014849.1  (499) IKSLIRLSQNSGVFIPIYPLLSEILTSTAFTKAPKKSPNLAAFDFEHNIKCTQAYLNTKIYQEGLSEQFVDLLGDYFALYCKNIASPELV
                    Consensus  (544) VRALTLLS STGTFIPVLPFILEIFQQVDFNRRPGR MSSKPINFSVILKLSK NLQEKAYRDGLVEQLYDLLLEYLH QAHSIAFPELV

                RBL=At3G55510  (506) TIPVMRLKKFHERSTMEGLKRVVKRFIEQVESNIEFVQRKFDD--VTFSPNDQQSADTFMQLEKQNANAPYTQYYQSII
                      At2g18220  (545) FIPTIRLRSFCKSTKAERFRKEMKQLISQIEANSEFVNKKRAL--IKFLPNDLAAESFLEDEKKA-GKTPLLQYAEIIR
          Chicken_NP_001026047  (534) LPTVIQLKSFLKECKIANYCKPIRQLLEKLQENSAYIASRRQQK--ATFGVASRESVEQWEKQVKE-EGTPLTKYYAQWK
            Cow_NP_001029498.1  (543) LPAVLQLKSFLRECKVANYCRQVRQLLEKVQENAEHIRSVRQK--VSFGVSDQRAVDAWEKRTRE-EGTPLTKYYSQWR
              Dog_XP_546728.2  (559) LPAVLQLKSFLRECKVANYCRQLRQLLEKVQENAEYICSRRQG--ASFSVADLHAVDTWEKQTRE-EGTPLTKYYNQWR
          Fruitfly_NP_610095.1  (565) VPTVMAIKTYLKECRNANYARKLKQLLEKIQESARFIEQQRGKSSVTFDIKDAQAVAAWEQQLRL-KRTPLDVYYASWL
             Human_NP_056473.1  (548) LPVVLQLKSFLRECKVANYCRQVQQLLGKVQENSAYICSRRQR--VSFGVSEQQAVEAWEKLTRE-EGTPLTLYYSHWR
            Mouse_NP_067278.1  (552) LPTVLQLKSFLRECKVANYCRQVRQLLEKVQENAQHIQSLRQS--ATFSVSDQMAVDAWEKQVRE-EGTPLTRYYGHWK
           Rat_NP_001029069.1  (445) LPTVLQLKSFLRECKVANYCRQVRQLLEKVQENAEHIRSLRQR--VTFSVSDQLAVDAWEKKVRE-EGTPLTRYYSHWK
            Yeast_NP_014849.1  (589) TPVIISLRRYIKTSTNVKLNKRLSTVVEKLNQNSTFIQEKRSD--VEFGPTNKSEVSRFLNDVAW-NKTPLGSYVAVQR
                    Consensus  (634) LP VLQLKSFLRECKVANYCRQVRQLLEKVQENAEFI SKRQK  VTF VSDQ AVDAWEK VRE EGTPLTKYYA WR
```

**Figure 2.** Structures of the *RBL*, *SQN*, and *ULT1* Genes and Mapping of the Allelic Mutations.

Multiple sequence alignment of RBL, At2g18820, yeast, and animal NOC2/UPF0120 domains.

**(A)** Genomic organization of *RBL* (At3g55510), *SQN* (At2g15790), and *ULT1* (At4g28190). The positions of the mutations are shown below the sequences. Stars indicate amino acid substitutions and triangle-shaped forms indicate T-DNA insertion. *RBL* is a single-copy gene and is predicted to consist of eight exons and encode a protein of 594 amino acids. *rbl-1* corresponds to the G-to-A transition at nucleotide position 22 relative to the translational initiation site that changes an Ala residue to a Thr residue. *rbl-2* (FLAG 299B04) corresponds to a T-DNA insertion in the promoter region,

**Table 1.** Floral Organ Number in *crc-1*, *rbl-1*, *sqn-4*, and *ult1-4* Single Mutants and in Double Mutants Generated in Pairwise Combinations

| | Sepal Number | Petal Number | Stamen Number | Primary Carpel Number | Flowers with Extra Organs inside the Primary Carpel (%) | |
|---|---|---|---|---|---|---|
| Wild type | 4 ± 0 | 4.01 ± 0.1 | 5.98 ± 0.2 | 2.01 ± 0.1 | 0 | $n = 100$ |
| *crc-1* | 4.04 ± 0.2 | 4,06 ± 0.24 | 5.80 ± 0.49 | 2 ± 0 | 0 | $n = 100$ |
| *rbl-1* | 4.01 ± 0.1 | 4.02 ± 0.14 | 5.99 ± 0.17 | 3.1 ± 0.56 | 0 | $n = 100$ |
| *sqn-4* | 4 ± 0 | 4 ± 0 | 6 ± 0 | 2.51 ± 0.52 | 0 | $n = 100$ |
| *ult1-4* | 4.48 ± 0.7 | 4.7 ± 0.86 | 6.05 ± 0.46 | 2.2 ± 0.2 | 4[a] | $n = 100$ |
| *rbl-1 sqn-4* | 4.02 ± 0.15 | 4.02 ± 0.2 | 6 ± 0.15 | 3.15 ± 0.31 | 100 | $n = 45$ |
| *rbl-1 ult1-4* | 4.86 ± 0.86 | 4.8 ± 0.86 | 6 ± 0 | 2.98 ± 0.14 | 90 | $n = 50$ |
| *sqn-4 ult1-4* | 5.96 ± 0.56 | 5.96 ± 0.58 | 6 ± 0 | 3 ± 0 | 100 | $n = 28$ |
| *crc-1 rbl-1* | ND | ND | ND | 3 ± 0.8 | 100 | $n = 120$ |
| *crc-1 sqn-4* | ND | ND | ND | 2.71 ± 0.76 | 86 | $n = 110$ |
| *crc-1 ult1-4* | 5.38 ± 0.93 | 5.37 ± 1 | 5.95 ± 0.52 | 2.63 ± 0.71 | 83 | $n = 115$ |

[a] Small carpeloid or stigmatoid tissues developing from the placenta.

Numbers given are the mean ± SE. P values for carpel number differences between the single mutants and the wild type are highly significant. These differences are not significant between *rbl-1* and all double mutants containing *rbl-1* but are between *sqn-4*, *ult-4*, and *crc-1* and the corresponding double mutants. Effect of *sqn-4*, *ult-4*, and *crc-1* mutations on primary carpel number is therefore additive. ND, not determined; $n$ = number of flowers counted.

mapped to At3g55510. *rbl-1* is caused by the replacement of an Ala residue by a Thr, eight amino acids downstream of the first Met (Figure 2A). Two additional alleles, *rbl-2* (FLAG 299B04; Institut National de la Recherche Agronomique, Versailles) and *rbl-3* (SALK 059.267; Figure 2A), were crossed to *crc-1*. The resulting *crc-1 rbl-2* double mutants developed indeterminate flowers (see Supplemental Figure 1A online), confirming *RBL* as At3g55510. *rbl-3* causes embryonic lethality with an arrest of embryo development at the heart stage (see Supplemental Figure 2 online). This suggests that *rbl-1* and *rbl-2* are partial loss-of-function alleles, and *rbl-1* reveals only one of RBL's functions. However, indeterminate flowers were also observed in *crc-1 rbl-3*/+ plants, implying a dose-dependent effect of the *rbl-3* mutation in a *crc* background. Database searches revealed one sequence similar to *RBL* in *Arabidopsis*: At2g18220. RBL and At2g18220 share 26% identity and 39% similarity over the full length of the proteins (see Supplemental Figure 3 online). Sequence analyses of RBL and At2g18220 recognized the conserved NOC2 domain, also known as UPF0120 domain (Figure 2B), located between amino acids 256 and 582 in RBL. This domain identifies an uncharacterized protein family and its name is based on yeast Noc2p (Milkereit et al., 2001), the founding member of the family. RBL and At2g18220 share 35% identity and 56% similarity over the NOC2 domain, and RBL and At2g18220 show 25 and 28% identity and 39 and 45% similarity, respectively, with the yeast NOC2 domain (Figure 2B). In yeast, the Noc2 protein is required for the maturation and intranuclear transport of the 60S ribosome subunit and pre-rRNA processing (Milkereit et al., 2001). *NOC2* was shown to be essential for embryonic development in *Caenorhabditis elegans* (Kamath et al., 2003) and zebra fish (Amsterdam et al., 2004). Interestingly, a human NOC2-containing protein has been identified as an inhibitor of histone acetyltransferase activity (Hublitz et al., 2005).

The second EMS-induced *crc* modifier was mapped to At2g15790, which corresponds to *SQN*, the *Arabidopsis* homolog of cyclophilin 40 (CyP-40; Berardini et al., 2001). The new allele, *sqn-4*, has a G-to-A transition that alters the donor-splicing site of the 7th intron (Figure 2A). To verify that the mutation indeed corresponds to the *SQN* locus, the double mutant was constructed with *crc-1* and another *sqn* allele, *sqn-5* (SALK 033.511; Figure 2A). *crc-1 sqn-5* was found to develop additional stamens and carpels inside the primary carpels (see Supplemental Figure 1B online). *SQN* is the only representative of

**Figure 2.** (continued).

531bp upstream the start codon (the right border insertion could not be mapped). *rbl-3* (SALK 059.267) contains a T-DNA insertion between positions 2109 and 2122 downstream the ATG, disrupting *RBL* in the 6th exon. *SQN* is predicted to consist of eight exons and encode a protein of 361 amino acids. *sqn-4* corresponds to a G-to-A transition in the 7th exon to the 7th intron splicing site. *sqn-5* (SALK 033.511) bears a T-DNA between positions 673 and 687 (15 bp deletion) downstream of the start codon, disrupting *SQN* in the 5th intron. The *ULT1* complete coding region is 714 bp in length and consists of three exons encoding a protein of 237 amino acids. *ult1-3* (SALK 0574.642) contains a T-DNA insertion in the first exon, 159 bp after the START codon. *ult1-4* contains a T-DNA inserted 95 bp upstream to the translational START site to 25 bp downstream to the translational STOP site. **(B)** The RBL NOC2/UPF0120 domain sequence (256 to 582 amino acids) is compared with the NOC2/UPF0120 domain sequences of *Arabidopsis* At2g18820 and of NOC2 proteins from chicken, cow, dog, fruitfly, human, mouse, rat, and yeast. Such a comparison shows that the NOC2/UPF0120 domains observed in RBL and At2g18220 proteins are significantly conserved. The alignment was done using VectorNTI 10.0.1 (Invitrogen). The black letters on a white background represent different residues. The black letters on a gray background represent conserved residues. The white letters on a black background represent identical residues. Arrowheads above RBL in **(A)** denote the position of the NOC/UPF0120 domain.

the CyP-40 family in *Arabidopsis* and is predicted to have a peptidyl-prolyl *cis-trans* isomerase activity domain.

The third *crc* modifier was induced by a T-DNA insertion (Eshed et al., 1999). Sequencing of the flanking regions indicated that the T-DNA disrupted At4g28190, corresponding to *ULT1* (Carles et al., 2005). Our mutation was therefore named *ult1-4*. In *ult1-4*, the borders of a T-DNA are inserted 95 bp upstream of the translational start site and 25 bp downstream of the stop codon (Figure 2A), resulting in a complete deletion of the coding sequence. RT-PCR experiments confirmed an absence of *ULT1* transcripts in *ult1-4* (see Supplemental Figure 4 online) that therefore corresponds to a null allele. Here, too, an additional *ult1* allele, *ult1-3* (SALK 074.642; Figure 2A), was crossed to *crc-1*, and the resulting double mutant presented the characteristic ''Russian doll'' gynoecium (see Supplemental Figure 1C online). *ULT1* encodes a small protein containing a SAND domain, located between the 18th and the 108th amino acid, and a Cys-rich region. ULT1 and the closely related ULT2 (At2g20825) are the only two SAND domain proteins in the *Arabidopsis* genome. The SAND domain is a specific DNA binding domain previously characterized in Sp100, AIRE-1, NucP41/75, and DEAF-1 proteins (Gibson et al., 1998).

According to their predicted sequences and motifs, RBL, SQN, and ULT1 control FM termination by seemingly unrelated mechanisms. Moreover, the binary interactions between RBL, SQN, ULT1, and CRC have been tested using the yeast two-hybrid technique, and no physical interactions have been observed (see Supplemental Figure 5 online).

### *RBL*, *SQN*, and *ULT1* Expression Patterns and Subcellular Localization of the Proteins

We used RT-PCR to determine the distribution of *RBL*, *SQN*, and *ULT1* mRNA transcripts in wild-type tissues (Figure 3A). The three genes are expressed in all tissues tested, the highest levels of expression being observed in tissues with cells undergoing division, especially in the inflorescence, and the lowest in old leaves, except for *SQN*, whose expression level remained constant during leaf development. Global expression data analyses (Digital Northern, Gene Chronologer, Gene Atlas, and Meta Analyzer; https://www.genevestigator.ethz.ch/at/) also indicated that the three genes are ubiquitously expressed, with higher expression levels during the flowering transition and during seed formation and at the rosette stage for *SQN*. We also analyzed the global expression data in homeotic flower mutant backgrounds (Wellmer et al., 2004) and found that *RBL*, *SQN*, and *ULT1* transcript levels were not altered in *ap1*, *ap2*, *ap3*, *pi*, and *ag* mutants.

We next performed in situ hybridization experiments to localize more precisely *RBL*, *SQN*, and *ULT1* transcripts during flower development. Regarding *ULT1*, we obtained similar flower expression patterns to those described by Carles et al. (2005). *RBL* expression can be detected throughout the iSAM and the FM at young stages 1 and 2 (Figure 3B). Later during flower development, the hybridization signal becomes weaker in differentiating organs and remains strong in the center of FM and young emerging primordia (Figures 3C to 3F). However, this apparent reduction of the signal is likely due to differences in cell density and size in differentiating organs compared with proliferating tissues, rather than to a decrease of *RBL* expression per se. In mature flowers (stages 11 to 13), a strong signal is detected in ovules (Figure 3G) and a weak one (possibly for the same reasons as those described above) in valves. Fusions of the β-glucuronidase (*GUS*) reporter gene downstream of *RBL* promoter sequences confirmed the ubiquitous expression patterns of *RBL* (Figures 3I to 3L). We did not manage to obtain detectable in situ hybridization signals with *SQN*, whose expression is likely very low and ubiquitous, making signals difficult to observe compared with the background. Fusions of the *GUS* reporter gene downstream of *SQN* promoter sequences indicate ubiquitous expression pattern (Figures 3Q to 3S), with the exception of anthers, which remained unlabeled in several independent transgenic lines.

To determine the in vivo subcellular localization of each protein, we generated transgenic plants stably expressing RBL-green fluorescent protein (GFP) and SQN-GFP fusion proteins under the control of the 35S promoter (Figures 3M and 3T, respectively) and the RBL-monomeric red fluorescent protein (mRFP) fusion protein under the control of its own promoter (Figure 3N). Transgenic plants expressing the SQN-GFP fusion protein under the control of its own promoter were also generated but did not provide detectable signals, likely because of the low expression level. Both *ProRBL:RBL-mRFP* and *ProSQN:SQN-GFP* constructs were able to complement the indeterminacy phenotype generated by the corresponding double mutant with *crc-1* (see Supplemental Table 1 online). Confocal microscopy observations were performed on roots and show that RBL is localized in the nucleus and SQN in the cytoplasm (Figures 3M, 3N, and 3T, respectively). Since expression levels of the fluorescent proteins were sometimes low (especially with the SQN-GFP construct), we also performed transient expression assays in tobacco (*Nicotiana benthamiana*) leaves using the same RBL- and SQN-GFP fusions. RBL is mainly localized in the entire nucleus (Figure 3P), and SQN is mainly localized in the cytoplasm (Figure 3U).

In summary, *RBL* and *SQN* seem to display ubiquitous expression patterns. RBL, SQN, and ULT1 are probably general regulators of development acting upstream of flower-specific genes to trigger more specific effects on FM termination.

### *WUS* and *CLV3* Expression Persists in the Center of the Floral Meristem in the *crc-1 rbl-1*, *crc-1 sqn-4*, and *crc-1 ult1-4* Double Mutants

To investigate the molecular basis of the indeterminacy in *crc-1 rbl-1*, *crc-1 sqn-4*, and *crc-1 ult1-4* backgrounds, we followed *WUS* and *CLV3* expression by in situ hybridization and with a *ProCLV3:GFP* reporter line, respectively.

In wild-type plants, *WUS* is not expressed at stage 6, after carpel primordia emerge (Mayer et al., 1998; Figure 4A). In each of the three double *crc-1 rbl-1*, *crc-1 sqn-4*, and *crc-1 ult1-4* mutants, during stage 6, a strong *WUS* expression is detected in the center of the dome that separates carpel primordia (Figures 4B to 4D). *WUS* expression remains detectable until much later stages (Figure 4E). The three double *crc-1 rbl-1*, *crc-1 sqn-4*, and *crc-1 ult1-4* mutants were crossed with the *ProCLV3:GFP*

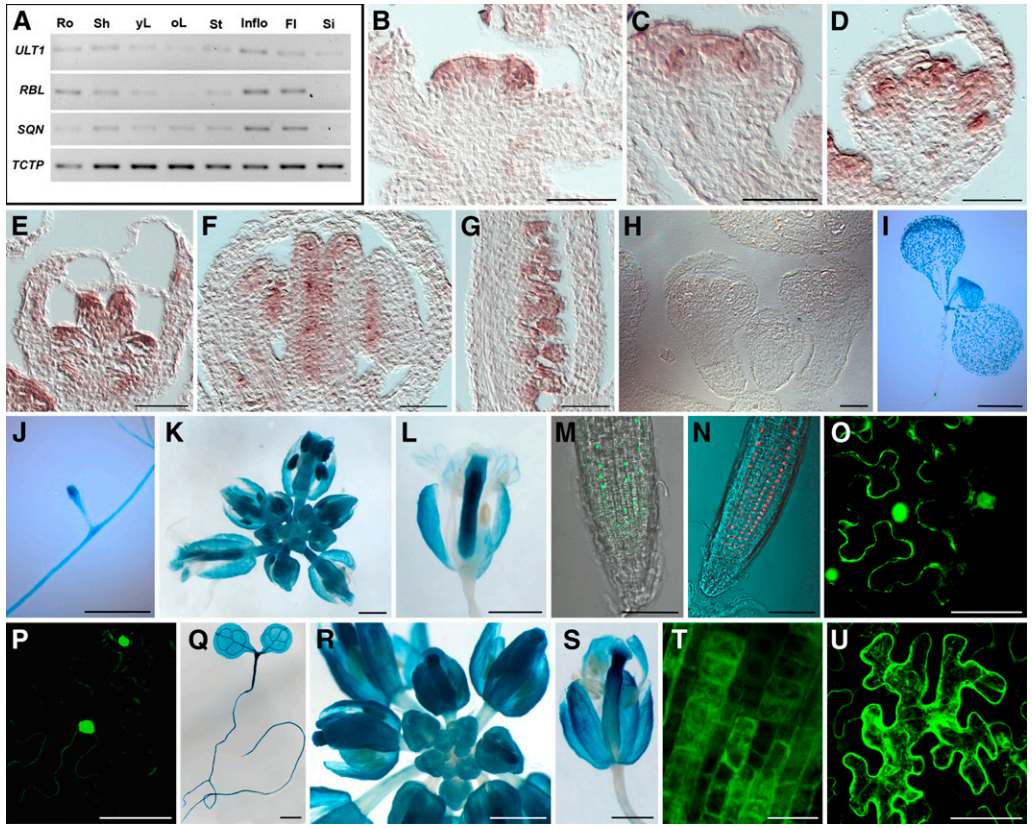


**Figure 3.** Expression Patterns of the Three Genes and Subcellular Localizations of RBL and SQN.

**(A)** RT-PCR analysis was performed on RNA extracts from wild-type Landsberg *erecta* (L*er*) tissues: roots (Ro), shoot (Sh), young leaves (yL), old leaves (oL), stem (St), inflorescence (Inflo = iSAM + young buds), flower (Fl), and silique (Si). *TCTP* (translationally controlled tumor protein; At3g16640) was amplified as a control (Szecsi et al., 2006).

**(B)** to **(G)** *RBL* expression pattern monitored by in situ hybridization on longitudinal sections of the iSAM **(B)**, flower buds at stages 3 to 4 **(C)**, stage 6 **(D)**, stage 7 **(E)**, stages 8 to 9 **(F)**, and ovules **(G)**. RBL mRNA is detected throughout the iSAM. The level of *RBL* expression is stronger in the center of flower buds and weaker in differentiating tissues.

**(H)** Control hybridization with *RBL* sense probe, showing no signal.

**(I)** to **(L)** Expression pattern of the GUS reporter gene cloned under the control of the *RBL* promoter. GUS is ubiquitously detected throughout plant development, in plantlets **(I)**, roots **(J)**, inflorescence **(K)**, and flowers **(L)**, with strong expression in the SAM.

**(M)**, **(N)**, and **(P)** RBL subcellular localization, using the *Prom35S:RBL-GFP* **(M)** and the *PromRBL:RBL-mRFP* **(N)** constructs in *Arabidopsis* roots (stable transgenics) and the *Prom35S:RBL-GFP* **(P)** construct in tobacco leaf cells (transient expression). RBL displays a nuclear localization.

**(O)** GFP expression pattern in tobacco cells infiltrated by the *Prom35S:GFP* construct as control.

**(Q)** to **(S)** Expression pattern of GUS cloned under the control of the *SQN* promoter (intergenic sequence). As above, GUS is ubiquitously detected in plantlets **(Q)**, inflorescence **(R)**, and flowers **(S)**.

**(T)** and **(U)** SQN subcellular localization using the *Prom35S:SQN-GFP* **(T)** construct in *Arabidopsis* root cells (stable transgenics) and the *Prom35S:SQN-GFP* **(U)** construct in tobacco leaf cells (transient expression). SQN is detected in cytoplasm.

Bars = 500 μm in **(I)** to **(N)** and **(Q)** to **(S)** and 50 μm in **(B)** to **(H)** and **(O)**, **(P)**, **(T)**, and **(U)**.

reporter line. Stereomicroscopy GFP observations of F2 plants, homozygous for both mutant alleles and containing the *CLV3* reporter construct, show that the apices of indeterminate flowers express *CLV3* (Figure 4F), thus confirming the maintenance of a bona fide meristematic activity.

### *SQN* and *ULT1* Promote *AG* Expression in an Inner Subdomain of Whorl 4

The prominent role of AG in the control of FM termination prompted us to monitor its expression pattern by in situ hybridization in the *crc-1 rbl-1*, *crc-1 sqn-4*, and *crc-1 ult1-4* backgrounds.

In the wild type, *AG* is uniformly expressed throughout the FM center from stage 3 and is restricted to the 3rd and 4th whorls from stage 5 onwards (Figures 5A to 5D). By contrast, *AG* expression seems to be downregulated in the very center of the FM from stage 3, in both *crc-1 sqn-4* (Figures 5E to 5H) and *crc-1 ult1-4* (Figures 5I to 5L). In the *crc-1 rbl-1* background, we were not able to observe obvious modifications of *AG* expression. Although *RBL* does not seem to affect the pattern of *AG* transcription, it could either positively and uniformly influence *AG*

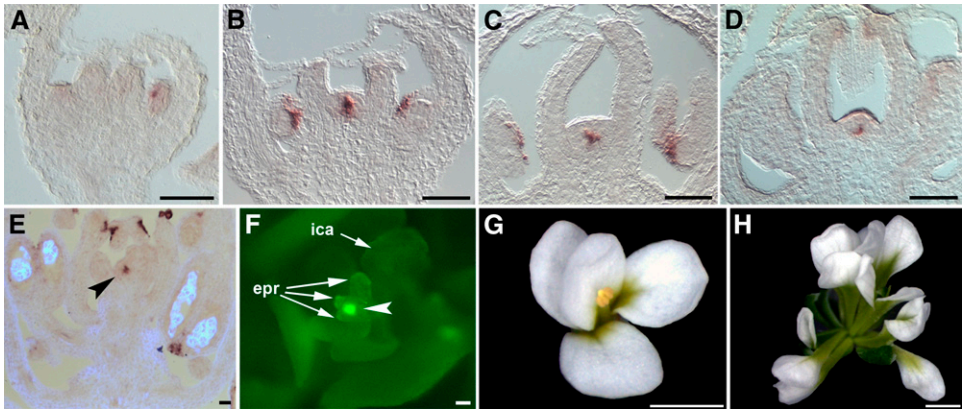


**Figure 4.** Analysis of *WUS* and *CLV3* Expression Patterns in *crc-1 rbl-1*, *crc-1 sqn-4*, and *crc-1 ult1-4* Double Mutant Backgrounds and Phenotypes of the *wus-1 rbl-1*, *wus-1 sqn-4*, and *wus-1 ult1-4* Double Mutants.

**(A)** to **(E)** *WUS* expression (monitored by in situ hybridization).
**(A)** L*er* flower, stage 6.
**(B)** *crc-1 rbl-1* flower, stage 6.
**(C)** *crc-1 sqn-4* flower, stage 8.
**(D)** *crc-1 ult1-4* flower, stage 8.
**(E)** *crc-1 sqn-4* flower, late stage. The black arrowhead points to the meristematic *WUS* expression domain. While *WUS* mRNA is not detected in the center of the FM at stage 6 in L*er* **(A)**, it remains detectable in *crc-1 rbl-1* **(B)**, *crc-1 sqn-4* **(C)**, and *crc-1 ult1-4* **(D)**, even at very late stages **(E)**.
**(F)** CLV3-GFP expression pattern in *crc-1 sqn-4* flower. The GFP expression in the center of the FM shows that *CLV3* also remains expressed long after stage 6 in the center of the FM of the double mutant (white arrowhead). This maintained meristem still produces ectopic primordia (epr) that develop into stamens and carpels (ica). Similar results were obtained with *crc-1 rbl-1* and *crc-1 ult1-4*.
**(G)** *wus-1 rbl-1* flower, identical to a *wus-1* flower (Laux et al., 1996), with four sepals, four petals, one to two stamens, and no carpel. *wus-1 sqn-4* flowers display a similar phenotype.
**(H)** *wus-1 ult1-4* flower. Similarly to *wus-1* and *wus-1 rbl-1*, *wus-1 ult1-4* flowers display one to two stamens and no carpel. However, they develop more sepals ($5.09 \pm 0.87$, $n = 45$) and petals ($5.84 \pm 1.3$, $n = 45$) than *wus-1*, suggesting that *ult1-4* influences sepal and petal numbers independently of *wus*.
Bars = 50 μm in **(A)** to **(F)** and 500 μm in **(G)** and **(H)**.

transcription throughout the FM center and young organ primordia or influence AG activity at a posttranscriptional level.

In conclusion, the downregulation of *AG* expression in the very center of the FM delimits a 4th whorl subdomain where specific regulatory pathways (involving *SQN* and *ULT1*) operate to control *AG* expression.

### *RBL*, *SQN*, and *ULT1* Redundantly Control FM Termination

We next evaluated the effects of each of the modifiers, alone or in combination, on FM determinacy. In each of the single mutants, the flowers produce supernumerary carpels (Table 1) that sometimes develop in the upper half of the gynoecium and therefore modify its morphology (Figure 6B). In addition, *ult1-4* shows a significant increase of sepal, petal, and stamen number (Table 1, Figure 6C). These data are in accordance with those reported by Berardini et al. (2001) for *sqn-1* and by Fletcher (2001) for other *ult1* alleles. Note that the gynoecia of the three mutants are also slightly shorter and wider than the wild type, but no additional whorls are produced inside. Thus, the three mutants exhibit mild effects on primary carpel number but show no alteration of FM termination.

Double mutants between *rbl-1*, *sqn-4*, and *ult1-4* were subsequently generated in pairwise combinations. In all of these double mutants, gynoecia are often borne on a gynophore and are shorter and wider compared with the wild type (Figure 6D). Some combinations also show increases in primary carpel numbers compared with single mutants (Table 1). In addition, gynoecia of all double mutants display reiterations of whorls of stamens, carpels, and sometimes petals inside the primary carpels, which are not observed in single mutants (Figure 6E). As observed in corresponding crosses with *crc-1*, the ectopic organs develop on an elongating axis that almost always grows from the base of the primary gynoecium. The phenotypic similarity (with the exception of the distal carpel fusion trait) of double mutants between *crc-1* and the identified modifiers and the modifiers themselves strongly suggests that *CRC* and its modifiers are required redundantly for FM termination.

In *rbl-1 sqn-4 ult1-4* triple mutant flowers, sepal and petal numbers are increased similar to that observed in *ult1-4* (Figures 6F and 6I). All triple mutant flowers display additional primary stamen whorls compared with the double mutants, but the strength of indeterminacy is variable between flowers along the inflorescence, with the strongest effects usually observed in the first flowers. In the weak phenotypes, the increase of primary stamen whorl number is moderate, while fused carpels enclosing extra floral organs (stamens and carpels) develop in the FM center (Figure 6F). In addition, chimeric stamen-petal organs regularly develop in place of the primary stamens (Figures 6G and 6H). In intermediate phenotypes, flowers do not display

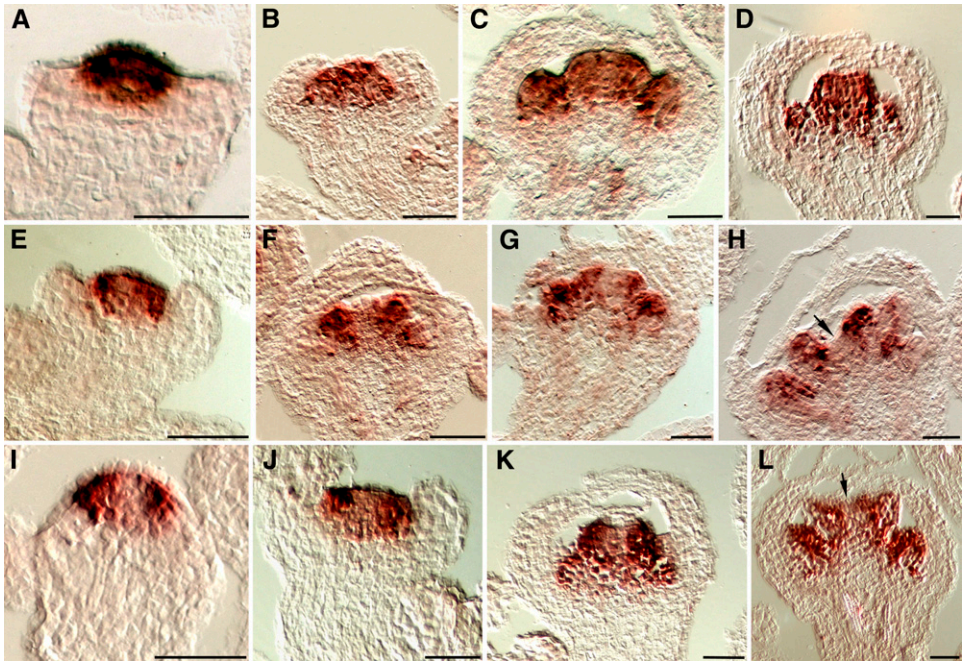


**Figure 5.** *AG* Expression Patterns in Wild-Type and *crc-1 sqn-4* and *crc-1 ult1-4* Double Mutant Backgrounds.

*AG* expression was monitored by in situ hybridization.
**(A)** to **(D)** *AG* expression pattern in L*er* flowers at stages 3 **(A)**, 4 **(B)**, and early and late 6 (**[C]** and **[D]**, respectively). *AG* expression is uniform throughout the FM center until stage 4 (**[A]** and **[B]**) and then throughout the 3rd and 4th whorls (**[C]** and **[D]**).
**(E)** to **(H)** *AG* expression pattern in *crc-1 sqn-4* flowers at stages 3 **(E)**, 5 **(F)**, 6 **(G)**, and 7 **(H)**.
**(I)** to **(L)** *AG* expression pattern in *crc-1 ult1-4* at stages 3 **(I)**, 4 **(J)**, 6 **(K)**, and 7 **(L)**. In both double mutants, *AG* expression is lower in the very center of the FM from stage 3. This region with a lower *AG* expression later defines a 4th whorl subdomain in the intercarpellary space (arrows in **[H]** and **[L]**). Bars = 30 μm.

fused carpels. Instead, reiterations of unfused carpel-like structures surrounding stamens are observed (Figure 6I). Chimeric stamen-carpel organs can also be observed in these flowers. These organs resemble stamens but bear ovules on the connective and display stigmatic papillae at their top (Figure 6J). Flowers showing a strong phenotype bear only stamens, organized in a spiral phyllotaxy and produced by an everlasting meristem at the center of mature flowers (Figures 6K and 6L).

In conclusion, our data show that *RBL*, *SQN*, and *ULT1* are genetically redundant and are involved in the control of FM termination. Their effects on FM termination depend on *WUS* activity since *wus-1* is epistatic to *rbl-1*, *sqn-4*, and *ult1-4* mutants: each double mutant develops one or two stamens and no carpels, similar to the *wus-1* single mutant (Figures 4G and 4H). Double mutant combinations between *rbl-1*, *sqn-4*, and *ult1-4* show the same type of indeterminacy observed in combinations with *crc-1* and show reiterations of ectopic stamens and carpels, suggesting that the effects of pairwise combinations of these mutants are limited to late events (from stage 6 onwards) of FM termination. By contrast, the triple mutant combination produces the completely new phenotype of a loss of FM termination with an expansion of whorl 3, giving rise to a spiral of stamens (Figures 6K and 6L). Thus, the simultaneous malfunctioning of these three genes has effects on earlier events (before stage 6) of FM termination compared with the pairwise combinations of these same mutations. The loss of FM termination, the development of chimeric petal/stamen organs, and the large increase of stamen number are reminiscent of some aspects of the *ag* and *sup* phenotypes and therefore suggest that *RBL*, *SQN*, and *ULT1* genes could function in both *AG* and *SUP* pathways.

### *rbl-1*, *sqn-4*, and *ult1-4* Reinforce the *ag* Phenotype

To further investigate the interactions of *RBL*, *SQN*, and *ULT1* with *AG*, we crossed *rbl-1*, *sqn-4*, and *ult1-4* to *ag-4* (weak allele [Sieburth et al., 1995]; Figures 7A to 7D, 7I, and 7J) and *ag-6* (strong allele; Figures 7E to 7J). *ag-6* results from a T-DNA insertion in *AG*, and protein gel blot analysis of total protein from wild-type and *ag-6* mutants with an AG-specific polyclonal antibody (Ito et al., 1997) demonstrated that the AG protein is not expressed in *ag-6*, thus confirming *ag-6* as a null allele.

First, *ag-4 rbl-1* double mutants develop flowers that resemble *ag-6* flowers (cf. Figures 7A, 7B, and 7E), whereas the *ag-4 sqn-4* double mutant flowers produce more organs than *ag-4* (cf. Figures 7A to 7C), and the *ag-4 ult1-4* double mutant develops flowers similar to *ag-4* flowers but with some of the stamens partially transformed into petals (cf. Figures 7A and 7D). The distinct enhancements of the *ag-4* phenotype therefore suggest that *RBL*, *SQN*, and *ULT1* all positively influence AG activity.

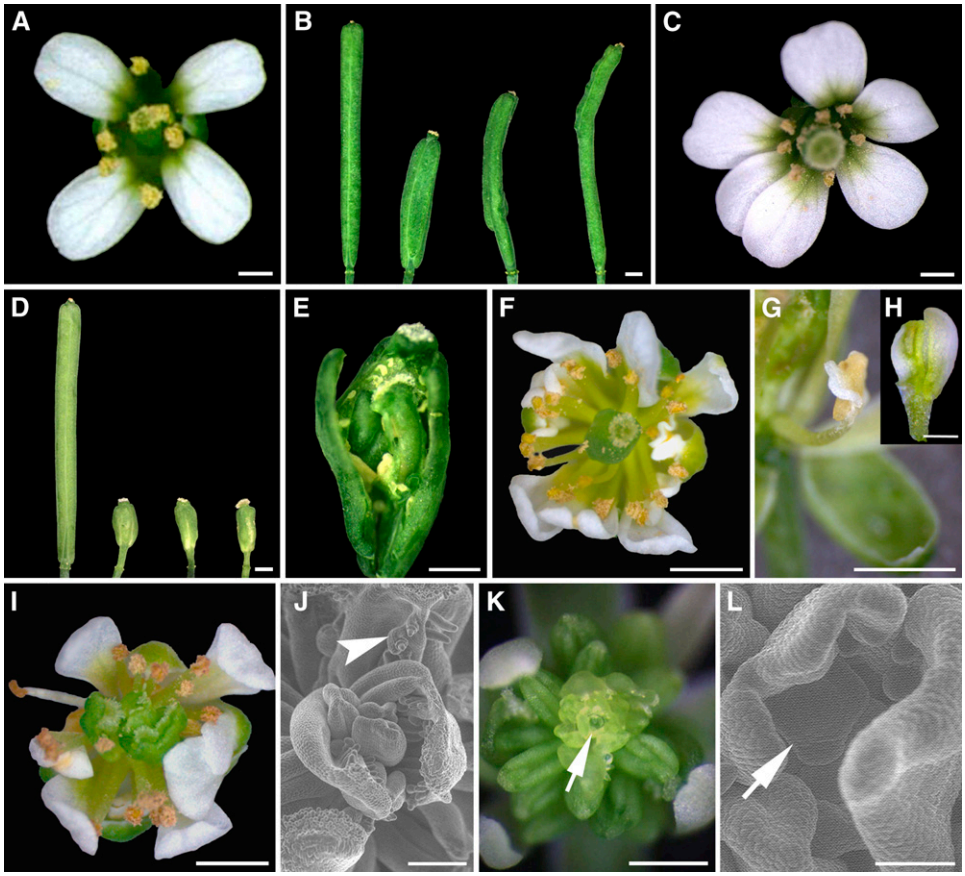


**Figure 6.** Phenotypes of the *rbl-1*, *sqn-4*, and *ult1-4* Single, Double, and Triple Mutants.

**(A)** L*er* flower.
**(B)** From the left to the right, siliques from L*er*, *rbl-1*, *sqn-4*, and *ult1-4* single mutants. Compared with the wild type, siliques from the single mutants display extra carpels that can develop in the upper half of the gynoecium.
**(C)** *ult1-4* flower, with extra petals.
**(D)** From the left to the right, siliques from L*er*, *rbl-1 sqn-4*, *rbl-1 ult1-4*, and *sqn-4 ult1-4* double mutants. Compared with L*er*, siliques from the double mutants are much shorter, develop extra carpels, and are borne by a gynophore.
**(E)** Dissection of *rbl-1 sqn-4* silique. Stamens and carpels are reiterated inside the primary carpels (similar results were obtained with *rbl-1 ult1-4* and *sqn-4 ult1-4*).
**(F)** to **(L)** Flowers of the *rbl-1 sqn-4 ult1-4* triple mutant.
**(F)** to **(H)** Weak phenotype. The flowers develop extra stamens and fused carpels that enclose extra floral organs. Chimerical petaloid stamens regularly develop in place of stamens in flowers of the *rbl-1 sqn-4 ult1-4* triple mutant (**[G]** and **[H]**).
**(I)** and **(J)** Intermediate phenotypes. The flowers reiterate whorls of stamens that eventually become carpelloid: they bear ovules (arrowhead) along the connective and stigmatic papillae at their top **(J)**.
**(K)** and **(L)** Strong phenotype. After the two first whorls, the flowers become totally indeterminate, with an indeterminate meristem (arrows) that produces only stamens following a spiraled phyllotaxy. **(J)** and **(L)** are scanning electron microscopy close-up views of **(I)** and **(K)**, respectively.
Bars = 500 μm, except in **(J)** and **(L)**, were bars = 80 μm.

In the progeny from the cross with *ag-6*, double mutants look only slightly different from *ag-6* (cf. Figures 7E and 7F). In *ag-6* flowers, the successive whorls of sepals are clearly recognizable and there are 10.22 ± 0.52 ($n = 23$) petals between the two first sepal whorls. In *ag-6 rbl-1* and *ag-6 sqn-4* flowers, there are 12.36 ± 1.19 ($n = 28$) and 12.03 ± 1.28 ($n = 32$) petals, respectively, before reaching the second whorl of sepals (Figure 7G). *ag-6 rbl-1* and *ag-6 sqn-4* therefore have phenotypes that resemble those of *ag-6 sup-1* (cf. Figures 7F and 7H). A weaker transformation was observed in *ag-6 ult1-4*, since 11.68 ± 0.82 ($n = 19$) petals were counted before reaching the second whorl of sepals whose transformation into petal is less pronounced.

Plants inferred to be heterozygous for *ag-6* or *ag-4* and homozygous for either *rbl-1*, *sqn-4*, or *ult1-4* display a floral formula identical to that of the *rbl-1*, *sqn-4*, and *ult1-4* single mutants, but the gynoecia are larger, borne on a short gynophore (Figure 7I), and enclose ectopic stamens and carpels (Figure 7J) produced from the center of the FM. While 100% ($n = 69$) of *ag-4*/+ *rbl-1* flowers are indeterminate, only 41.6% ($n = 100$) of *ag-4*/+ *sqn-4* and 31.7% ($n = 124$) of *ag-4*/+ *ult1-4* are.

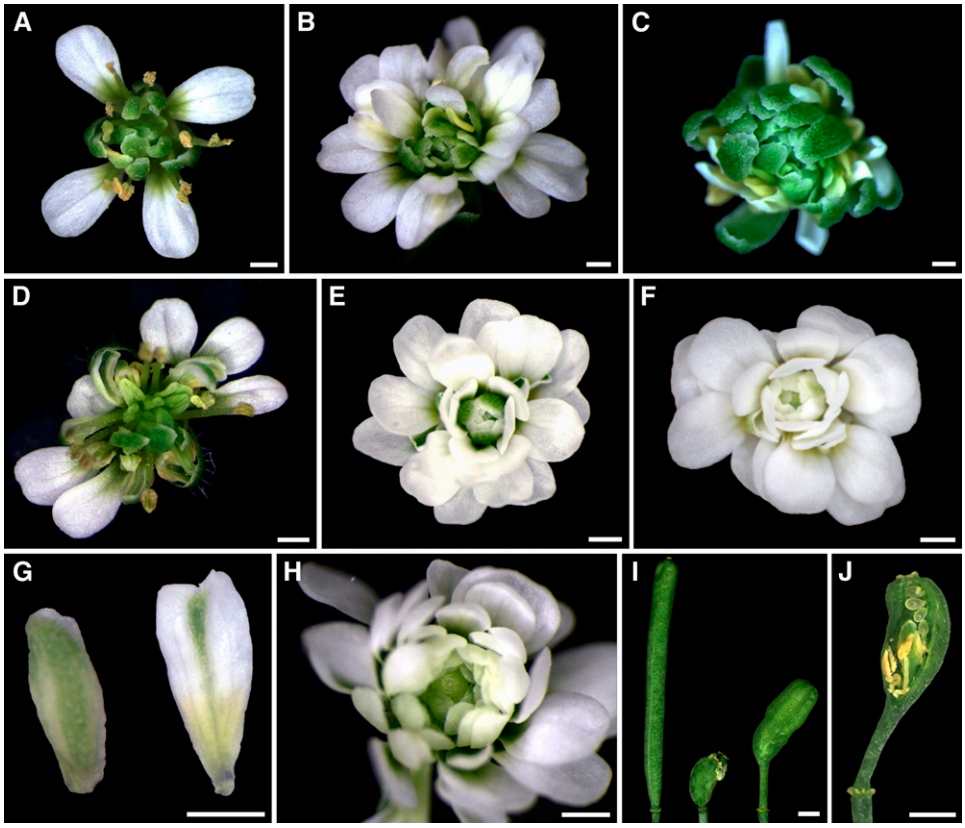


**Figure 7.** Phenotypes of *ag-4* and *ag-6* Single Mutants and of *ag rbl-1*, *ag sqn-4*, and *ag ult1-4* Double Mutants.

**(A)** *ag-4* (weak allele) flower.
**(B)** *ag-4 rbl-1* flower. Successive whorls of petals (with few remaining stamens) alternate with whorls of sepals. This flower resembles *ag-6* flowers.
**(C)** *ag-4 sqn-4* flower. This flower develops more organs than *ag-4* but does not show homeotic transformations.
**(D)** *ag-4 ult1-4* flower. This flower resembles *ag-4* flowers but also displays some partial stamen-to-petal transformations.
**(E)** *ag-6* (strong allele) flower.
**(F)** *ag-6 rbl-1* flower (we observed a similar phenotype with *ag-6 sqn-4*). Successive whorls of petals, without obvious alternating sepals, make *ag-6 rbl-1* flower different from *ag-6* flowers but similar to *ag-6 sup-1* flower.
**(G)** Second ring sepals from *ag-6 rbl-1* (right) and *ag-6* flowers (left). The *ag-6 rbl-1* ones are petaloid compared with the *ag-6* ones.
**(H)** *ag-6 sup-1* flower. Such a flower produces only petals, after a single whorl of sepals.
**(I)** From the left to the right, siliques from L*er*, *crc-1 rbl-1*, and *ag-4*/+ *rbl-1* double mutants (similar phenotype was observed with *ag-4*/+ *sqn-4* and *ag-4*/+ *ult1-4*). *ag-4*/+ *rbl-1* siliques are shorter than L*er* siliques and are borne by gynophores.
**(J)** Dissection of an *ag-4*/+ *rbl-1* silique. Extra floral organs develop inside primary carpels. For **(I)** and **(J)**, crosses with *ag-4* and *ag-6* give similar results. Bars = 500 μm.

Such results show that *rbl-1*, *sqn-4*, and *ult1-4* mutations enhance, to somewhat different degrees, the *ag-4* phenotype and, therefore, that *RBL*, *SQN*, and *ULT1* play partially redundant roles in AG activity. However, crosses with *ag-6* suggest that *RBL*, *SQN*, and, to a lesser extent, *ULT1* also mediate flower determinacy through an additional pathway that could involve *SUP* since phenotypes of *ag-6 rbl-1* and *ag-6 sqn-4* have attributes of those of *ag-1 sup-1* (Schultz et al., 1991; Bowman et al., 1992).

### *rbl-1*, *sqn-4*, and *ult1-4* Mutations Increase the *sup-1* Phenotype

The spirally initiated stamens observed in *rbl-1 sqn-4 ult1-4* and the *ag-1 sup-1*-like phenotype (Bowman et al., 1992), mimicked by *ag-6 rbl-1* and *ag-6 sqn-4*, prompted us to evaluate *RBL*, *SQN*, and *ULT1* functions with respect to SUP activity. *rbl-1*, *sqn-4*, and *ult1-4* mutants were therefore crossed with *sup-1*.

Compared with the wild type, *sup-1* produces more stamens and fewer carpels that are often staminoid (Figure 8A, Table 2; Bowman et al., 1992). The increase in floral organ number results from a delayed termination of the FM due to a delay of the extinction of *WUS* expression in the center of the FM (Figures 8B and 8C). Remarkably, *sup-1 rbl-1* flowers display everlasting meristems that indefinitely produce stamens in a spiral phyllotaxy (Figures 8D and 8E, Table 2). *sup-1 sqn-4* flowers also possess many more stamens than *sup-1* (Table 2), but the flowers produce a few unfused stamen-carpel organs at their center (Figures 8F and 8G), indicating a strongly delayed

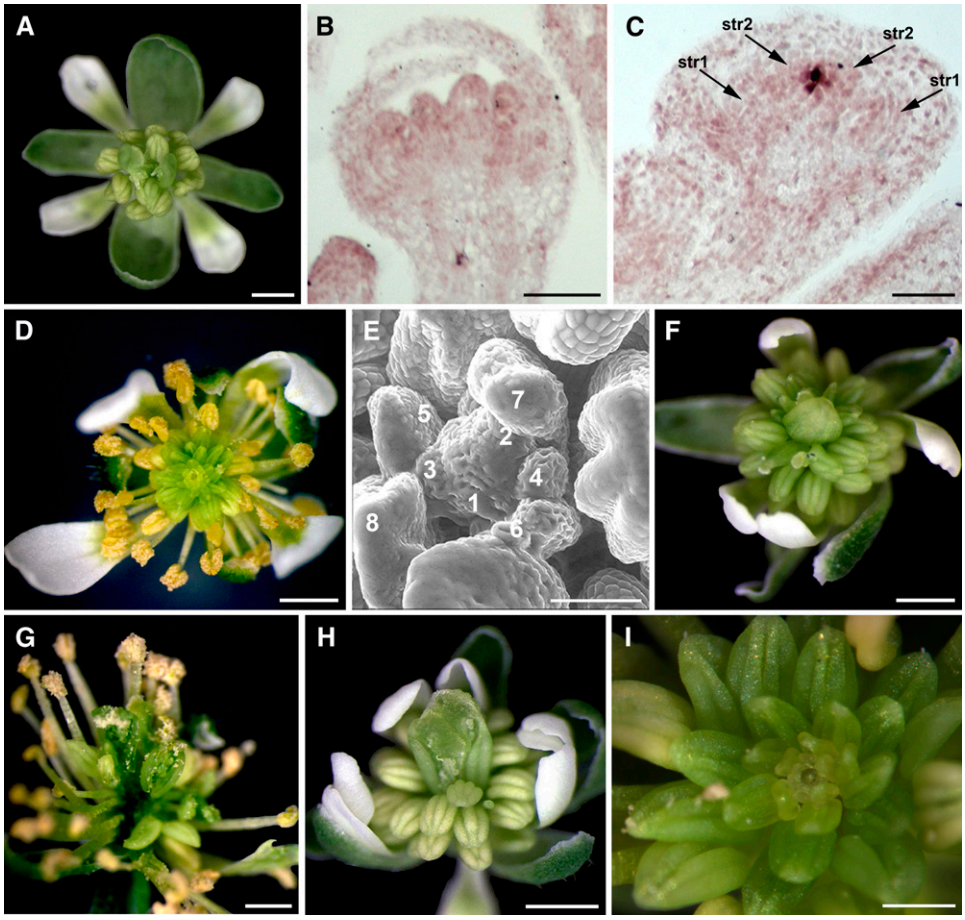


**Figure 8.** Phenotypes of *sup-1 rbl-1*, *sup-1 sqn-4*, *sup-1 ult1-4*, and *sup-1 ag-4* Double Mutants.

Analysis of *WUS* expression patterns in *sup-1*.
**(A)** *sup-1* flower.
**(B)** and **(C)** *WUS* expression (monitored by in situ hybridization). While *WUS* mRNA is not detected in L*er* FM at stage 6 **(B)**, it remains detectable in *sup-1* **(C)** at a similar or slightly older stage, when two consecutive rows of stamen (str1 and str2) are produced in the FM center.
**(D)** *sup-1 rbl-1* double mutant flower. The flower does not develop carpels but only stamens.
**(E)** Scanning electron microscopy magnification of the center of a *sup-1 rbl-1* double mutant flower. Stamens are produced by an everlasting meristem following a spiraled phyllotaxy. Numbers correspond to the successive primordia.
**(F)** and **(G)** Young and old flower, respectively, of a *sup-1 sqn-4* double mutant. Flowers produce a very high number of stamens, but end with unfused chimerical stamen-carpel organs.
**(H)** *sup-1 ult1-4* double mutant flower. The number of stamens produced is lower than in *sup-1 rbl-1* and *sup-1 sqn-4* and flower ends with unfused chimerical stamen-carpel organs.
**(I)** *sup-1 ag-4* double mutant flower. The flower does not develop carpels but only stamens following a spiraled phyllotaxy, thus mimicking *rbl-1 sup-1*.
Bars = 500 μm in **(A)**, **(D)**, and **(F)** to **(H)**, 200 μm in **(I)**, and 50 μm in **(B)**, **(C)**, and **(E)**.

termination. In *sup-1 sqn-4*, stamen phyllotaxy is spiral in the first five flowers and then becomes more whorled. Enhancement of the *sup-1* phenotype is less pronounced in the *ult1-4* background, where only additional stamens are produced compared with *sup-1* (Figure 8H, Table 2).

To test whether the enhancement of the *sup-1* phenotype by *rbl-1*, *sqn-4*, and *ult1-4* could be due to a slight decrease of AG function compared with the *sup-1* single mutant, we generated the *sup-1 ag-4* double mutant. As shown in Figures 8I, *sup-1 ag-4* flowers are indeterminate and produce an indefinite number of stamens in a spiral phyllotaxy, thus mimicking *rbl-1 sup-1*, and also the strong *rbl-1 sqn-4 ult1-4* phenotypes.

These data suggest that *rbl-1*, *sqn-4*, and, to a lesser extent, *ult1-4* increase the *sup-1* phenotype by decreasing AG function. However, the fact that the *rbl-1 sqn-4 ult1-4* triple mutant and the *sup-1 ag-4* double mutant produce indistinguishable indeterminate male flowers suggests that both AG and SUP activities are modified in *rbl-1 sqn-4 ult1-4.*

**Table 2.** Floral Organ Number in Single *sup-1* and Double *sup-1 rbl-1*, *sup-1 sqn-4*, and *sup-1 ult1-4* Mutants

| | Sepal Number | Petal Number | Stamen Number | Carpel Number | |
|---|---|---|---|---|---|
| Wild type | 4 ± 0 | 4.05 ± 0.05 | 5.97 ± 0.25 | 2.01 ± −0.15 | $n = 100$ |
| *sup-1* | 4.03 ± 0.25 | 4.55 ± 0.3 | 9.59 ± 1.58 | 0.8 ± 0.7 | $n = 100$ |
| *sup-1 rbl-1* | ND | ND | ∞[a] | – | |
| *sup-1 sqn-4* | ND | ND | >40[b] | 1.71 ± 0.96[c] | $n = 30$ |
| *sup-1 ult1-4* | 5.63 ± 1.16 | 6.1 ± 1.18 | 16.33 ± 2.82[b] | 0.95 ± 0.85 | $n = 30$ |
| *sup-1 ag-4* | ND | ND | ∞[a] | – | |

[a] Spiraled.
[b] On several whorls.
[c] Carpeloid stamens.
Numbers given are the mean ± SE. ND, not determined; $n$ = number of flowers counted.

### Mutations in B Class Genes Do Not Significantly Modify Floral Indeterminacy Levels Observed in the *crc-1 rbl-1*, *crc-1 sqn-4*, and *crc-1 ult1-4* Backgrounds

Previous data showed that each *crc* modifier in the *crc* background produces extra stamens inside gynoecia (Figure 1), implying that B class genes are reactivated in the FM center. To evaluate whether ectopic expression of B class genes influences FM indeterminacy in our mutant backgrounds, we introduced *pi-1* and *ap3-3* mutations into each of the *crc-1 rbl-1*, *crc-1 sqn-4*, and *crc-1 ult1-4* double mutants.

In B class single mutants, petals and stamens are transformed into sepals and carpels, respectively, and floral growth is determinate (Figures 9A and 9B; Bowman et al., 1989). In triple mutants (Figures 9C and 9D), floral organ identities are modified similarly to the *ap3-3* and *pi-1* single mutants, but FM growth remains indeterminate similar to the *crc-1 rbl-1*, *crc-1 sqn-4*, and *crc-1 ult1-4* double mutants. Since all triple mutants behave similarly (only two examples are given in Figure 9), we conclude that B class genes are not essential in promoting indeterminacy in *crc-1 rbl-1*, *crc-1 sqn-4*, and *crc-1 ult1-4* mutant backgrounds or that effects of B class mutations on FM termination depend on *AG*, as proposed from previously reported data (Bowman et al., 1989; Schultz et al., 1991; Sakai et al., 2000).

## DISCUSSION

Our results address the regulation of the switch from indeterminate to determinate growth during flower development. We report on three genes, *RBL* (a newly discovered and cloned gene), *SQN* (to which we assign a new function), and *ULT1*, which redundantly control FM termination. As single mutants, these genes have minor effects on carpel number, but when combined with each other or with mutations in *AG*, *SUP*, and *CRC*, they trigger a strong and persistent FM indeterminacy with the development of extra floral whorls. These phenotypes have been categorized into two different temporal classes (Figure 10A). We discuss the fact that these two classes reveal a continuous control on FM termination, which is initiated at stages 3 to 4 and maintained through stage 6 and beyond. Our data also point to the existence of an inner 4th whorl subdomain, which keeps a stem cell identity and maintains a meristematic potential, as distinct from the remainder of the 4th whorl, which is competent to produce carpel primordia. We suggest that a decrease of *AG* expression in this inner 4th whorl subdomain is sufficient to disrupt FM termination. However, we discuss why a decrease of AG activity alone is not sufficient to explain all phenotypes. Finally, we argue that *RBL*, *SQN*, and *ULT1* features make these genes candidates for contributors to floral developmental homeostasis.

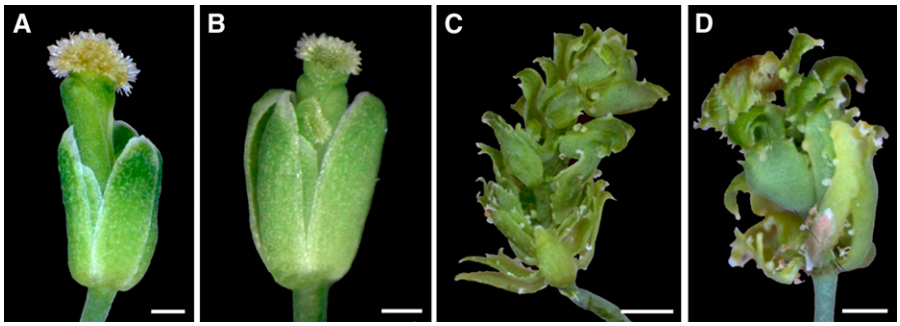


**Figure 9.** Phenotypes of Triple Mutants Combining *crc-1 rbl-1*, *crc-1 sqn-4*, or *crc-1 ult1-4* and *ap3-3* or *pi-1* Mutations.

**(A)** *ap3-3* flower.
**(B)** *pi-1* flower.
**(C)** and **(D)** Flowers from *crc-1 rbl-1 pi-1* and *crc-1 ult1-4 ap3-3* triple mutants, respectively. The triple mutant flowers are still strongly indeterminate and reiterate a high number of carpels.
Bars = 500 μm.

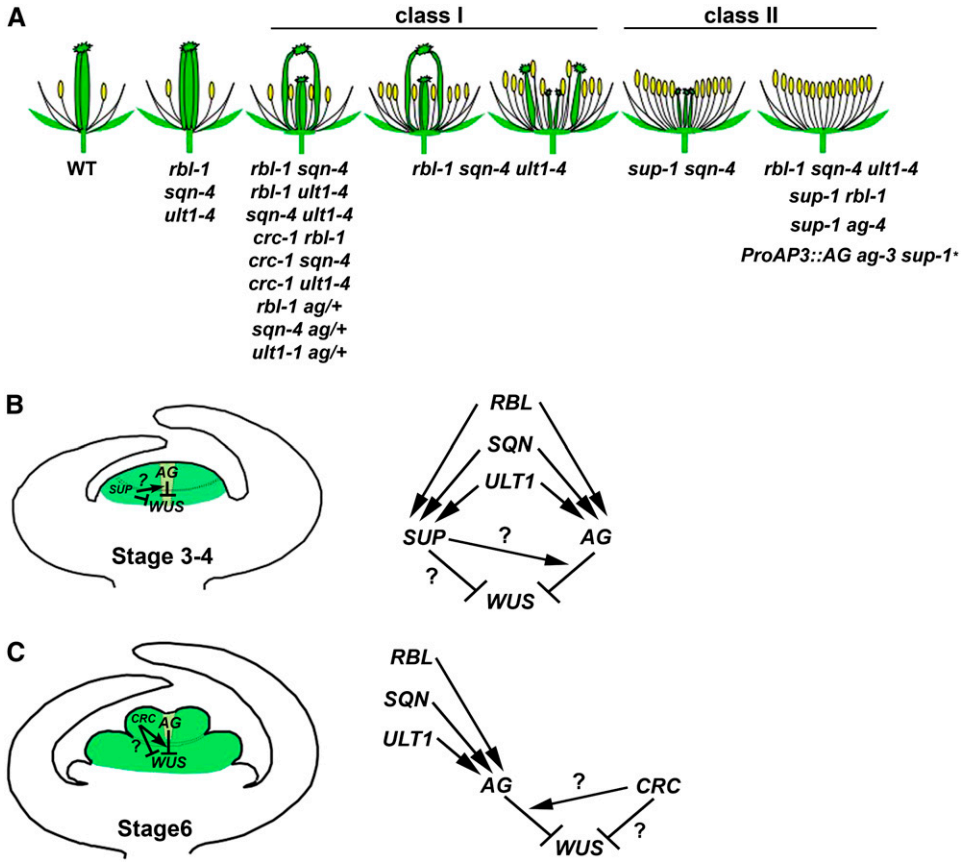


**Figure 10.** Model for *RBL*, *SQN*, and *ULT1* Action in the Spatial and Temporal Control of FM Determinacy.

**(A)** Sketch summarizing the phenotypes of flowers in different mutant backgrounds. Genotypes are indicated under the schemes. Class I groups together mutants that exhibit reiterations of stamens and carpels inside the primary carpels. Such FM indeterminacy is mainly due to a recurrent reset of the FM identity and results from events at stage 6 and beyond. Class II groups together mutants that exhibit an increase of primary stamen number. These mutants display a strong expansion of whorl 3, which, in the most extreme cases, gives rise to a spiral of stamens. Such a phenotype suggests that Class II type of indeterminacy results from earlier events, starting at stages 3 to 4.

**(B)** and **(C)** Stage 4 and 6 situations, respectively. *AG* expression domain is colored in green, with the inner subdomain, where *AG* is underexpressed in *crc-1 sqn-4* and *crc-1 ult1-4* backgrounds (Figure 5), in light green.

**(B)** At stage 4, we propose that *AG* and *SUP* both promote FM termination by repressing *WUS* expression (probably indirectly for *SUP*, by preventing B class gene expression in the center of the FM). This process corresponds to the early events of FM termination. We also propose that mutations in *RBL*, *SQN*, and *ULT1* decrease both AG and SUP activities in the FM center and thus result in Class II phenotypes.

**(C)** At stage 6, *AG* promotes FM termination by further repressing *WUS* expression. *CRC* also contributes (directly or indirectly) to FM termination, very likely, in an *AG*-independent manner. These events correspond to the late events of FM termination. We propose that AG activity therefore needs to be maintained in the inner 4th whorl subdomain for a persistent repression of the FM indeterminacy potential and that *RBL*, *SQN*, and *ULT1* appear to be required in this process.

### *RBL*, *SQN*, and *ULT1* Promote FM Termination from Stages 3 to 4 on and Maintain the Repression of a Meristematic Activity in the Center of the FM at Stage 6 and Beyond

The first class of phenotypes, observed in pairwise combinations of *rbl-1*, *sqn-4*, *ult1-4*, and *crc-1* (Class I; Figures 1, 6, and 10A), groups together flowers that show reiterations of stamens, carpels, and occasionally petals inside the primary carpels. Since reiterations are produced after the formation of the primary carpels, we estimate that they result from events at stage 6 and beyond. In addition, the identity of reiterated organs indicates a recurrent resetting of the FM identity after each carpel whorl. Our data therefore suggest that after primary carpels have been initiated as lateral organs on the floral axis (Bossinger and Smyth, 1996), a meristematic potential persists in the intercarpellary space. This would suggest that, in the wild type, stem cells are not entirely consumed to build carpels but rather transiently persist in a repressed state, with *RBL*, *SQN*, and *ULT1* playing a role in this process.

Flowers from the second class (Class II; Figures 6, 8, and 10A) show an increase of organ or whorl numbers in one or several of the primary floral organ domains. The strongest phenotype observed in this class, shown by the *rbl-1 sqn-4 ult-1* and the

*sup-1 rbl-1* mutant combinations, results in spirally indeterminate male flowers due to an expanding whorl 3. Unlike Class I, Class II phenotypes do not result from the recurrent resetting of the FM identity but rather from its maintenance with a continuing 3rd whorl identity. This indicates that indeterminacy takes place at an earlier stage in Class II mutants than in Class I. Since the reduction of *AG* expression in the very center of the FM is observed from stages 3 to 4 onward (Figure 5) and extra stamen development in *sup* mutants results from alteration to the whorl 3/4 boundary from stage 4 onward (Sakai et al., 1995, 2000), we propose that Class II phenotypes represent events occurring at stages 3 to 4.

The two phenotypic classes are arbitrary and, as suggested by Figure 10A, the phenotypic transitions within and between the two classes are progressive. The phenotypes therefore denote a continuum and strongly suggest that FM termination, once initiated at stages 3 to 4, needs to be continually maintained after all primary flower organs have been initiated, including carpels. However, the two classes have been instrumental in dissecting out the spatio-temporal control of FM termination, as discussed below.

### *RBL*, *SQN*, and *ULT1* Promote AG Function in FM Termination

Class I phenotypes result from a reduction of *AG* expression mainly in the intercarpellary space (Figures 5 and 10C). This is consistent with the transient reduction of *AG* expression previously observed in indeterminate *ult1-1* (Fletcher, 2001) and *clv1* (Clark et al., 1993) mutants and also with the Class I–like phenotypes generated in *AG* antisense experiments (Type III phenotypes in Mizukami and Ma, 1995). Interestingly, FM proliferation and floral reversion observed in *Impatiens* also correlate with an absence of *AG* expression in the central proliferating meristem (Chiurugwi et al., 2007). Class I phenotypes, however, differ from the one resulting from a lack of *AG* expression in the entire 4th whorl (*ProAP3:AG ag-3* plants; Jack et al., 1997). The latter is also indeterminate but does not produce carpels. Our data therefore restrict the domain where AG activity is necessary for the maintenance of FM termination to the intercarpellary space and show that *SQN* and *ULT1*, and probably *RBL*, are jointly required to promote *AG* activity in this domain (Figure 10C). Since *AG* expression is activated by *WUS* in a feedback loop (Lenhard et al., 2001; Lohmann et al., 2001) and *wus-1* is epistatic to *rbl-1*, *sqn-4*, and *ult1-4* (Figure 4), *RBL*, *SQN*, and *ULT1* could function downstream of *WUS* in the activation of *AG* in the center of the FM.

The two distinct functions of AG, organ identity and FM termination, therefore seem to correspond to distinct domains of expression, the 3rd whorl and the outer 4th whorl subdomains and the inner 4th whorl subdomain, respectively. Spatial determinants defining this last domain remain to be identified.

In addition, Class I mutants confirm the function of *CRC* in FM termination (Figures 1 and 10C) proposed by Alvarez and Smyth (1999), based on the fact that *crc-1 spt-2* and especially *crc-1 ag-1*/+ double mutants develop supernumerary whorls internal to the primary carpels. Similar to *AG*, *CRC* is therefore involved both in carpel identity (polarity, size, and distal fusion; Alvarez and Smyth, 1999; Eshed et al., 1999) and FM termination. However, the molecular role of *CRC* in this last regulatory network remains elusive. While it has been shown that *CRC* expression depends upon AG activity (Gomez-Mena et al., 2005; Lee et al., 2005), no data reported to date have shown the converse. That would suggest that CRC and AG influence floral termination through independent pathways, in agreement with the lack of *CRC* expression at the center of the stage 6 FM.

Class II phenotypes are also very likely to result from a reduction of AG activity in the inner 4th whorl subdomain, since reiterated organs produced on the flanks of the FM are stamens and occasionally carpels, and no phenotypes similar to strong *ag* alleles were generated in *rbl-1 sqn-4 ult1-4* and *sup-1 rbl-1* combinations (Figures 6, 8, and 10B). However, *AG* misregulation alone cannot explain the Class II phenotypes: strong indeterminacies observed in *ag* have not been associated with such an extended 3rd whorl (Bowman et al., 1989; Mizukami and Ma, 1995; Sieburth et al., 1995; Chuang and Meyerowitz, 2000). One hypothesis is that Class II phenotypes result from the down-regulation of both *SUP* and *AG* at stages 3 to 4, corresponding to the onset of their activities (Yanofsky et al., 1990; Schultz et al., 1991; Bowman et al., 1992; Sakai et al., 2000). Several observations support this hypothesis. First, we observed an increase of primary stamen number in the weak and moderate phenotypes of *rbl-1 sqn-4 ult1-4* (Figure 6). Second, the *ProAP3:AG ag-3 sup-1* mutant (Jack et al., 1997) and the *ag-1*/+ *sup-2* (Schultz et al., 1991) and *ag-4 sup-1* double mutants (Figure 8) display completely indeterminate male flowers, similar to the strong Class II phenotype (Figure 10A). Third, *ag-6 rbl-1* and *ag-6 sqn-4* display an *ag-6 sup-1*–like phenotype (Figure 7), with both phenotypes resembling the strong Class II phenotype (except for the phyllotaxy) with indeterminacy due to an expanded 3rd whorl, stamens being transformed into petals because of the strong *ag-6* allele. Our data highlight the convergence of AG and SUP pathways to control FM termination, as recently discussed by Sablowski (2007), and further support earlier data on the synergistic action of AG and SUP on FM determinacy (Schultz et al., 1991; Bowman et al., 1992). *RBL*, *SQN*, and, to a lesser extent, *ULT1* appear to be part of this flower termination regulatory pathway (Figure 10B).

Recently, it has been shown that ectopic expression of miR172-resistant *AP2* triggers floral indeterminacy with a phenotype similar to our strong Class II flowers (Zhao et al., 2007). Interestingly, the authors propose that this is due to a decrease in *AG* and *CLV* expression, together with an ectopic expression of *PI* in the center of the FM. Our data are consistent with this regulatory scheme, and effects of mutations in *RBL* and *SQN* on *AP2* and *CLV* activities deserve to be tested. However, the authors claimed that the shift of the inner boundary of B class gene expression toward the center of the FM, observed in the miR172-resistant *AP2* lines, does not depend on *SUP* activity but rather on the decrease of *AG* expression in the center of the FM. In our case, it seems that the Class II phenotype is unlikely to result from *AG* and *CLV* misregulation alone.

Together, our results, and the results of others, suggest that FM termination is based on a spatial and temporal sequence of events operating in the FM center (Figures 10B and 10C). The initiation phase (from stages 3 to 4) appears to require *AG* and

*SUP* activities. The maintenance phase (up to and beyond stage 6) appears to require *AG*, *CLV*, and probably *CRC* activities. Based on our results, we propose that RBL, SQN, and ULT1 are factors required during both early and late steps of the FM termination process (Figure 10).

### *RBL*, *SQN*, and *ULT1* Largely Contribute to Flower Termination Homeostasis

The range of floral indeterminacy phenotypes reported here might also have evolutionary implications since they illustrate phenotypic variations and transitions observed between flowers of the same family or during the course of evolution (Ronse de Craene, 2004; Baum and Hileman, 2006; Endress and Doyle, 2007). For instance, the combination of *sup-1* and *rbl-1* transforms a hermaphrodite whorled and determinate flower into a unisexual male, spiraled, and indeterminate flower. The mutant mimics the hypothetical angiosperm male ancestor flower, according to the out of male (Theissen et al., 2002) and the mostly male (Frohlich, 2002) theories. In addition, several Class I flowers display elongated internodes, an ancestral trait that tends to be repressed in the course of evolution, likely because of its lower reproductive fitness (Baum and Hileman, 2006). The fact that internode elongation only occurs between reiterated organs suggests that floral axis compaction and the competence for FM termination are linked in *Arabidopsis*.

The range of phenotypes also illustrates the consequences of a decreased floral developmental homeostasis. Floral developmental homeostasis corresponds to the tendency of angiosperms to make more uniform flowers (fixed number of parts developing in the right position), in spite of mutations and fluctuating environments (Frohlich, 2006). Core eudicots show more floral developmental homeostasis than many groups, such as *Ranunculaceae* (*Aquilegia* sp, *Helleborus foetidus*) or *Magnoliaceae* (*Magnolia* sp). These other groups have less uniform numbers of whorls and parts per whorl, similar to our mutants. It is conceivable that the evolution of enhanced developmental homeostasis in core eudicots was partly due to functions provided by *RBL*, *SQN*, and *ULT1* and that these genes might have played some indirect role in the great success of the core-eudicot clade.

## METHODS

### Plant Growth, Crosses, and Line Isolations

All mutants are in the L*er* ecotype background with the exception of the *ult1-3* (SALK 074.642), *crc-8* (SALK 065.539), *sqn-5* (SALK 033.511), *rbl-3* (SALK 059.267), and *rbl-4* (SALK 071.349) allelic lines that are in the Columbia-0 (Col-0) background and the *rbl-2* (FLAG 299B04) allelic line that is in the Wassilewskija background. Allelic lines were obtained from the Nottingham Arabidopsis Stock Centre (SIGnAL T-DNA-Express, http://www.arabidopsis.org) or the Institut National de la Recherche Agronomique, Versailles (*rbl-2*; http://dbsgap.versailles.inra.fr). *ag-1*, *ag-4*, *sup-1*, and the reporter line *ProCLV3:GFP* were provided by E. Meyerowitz (California Institute of Technology) and *wus-1* by T. Laux (University of Freiburg, Germany). *ag-6* is a new strong allele of *ag* resulting from a T-DNA insertion in *AG*.

Plants were grown in soil, first for 15 d under short-day conditions (10 h cool white fluorescent light; 10,000 lux luminosity; 55 to 80% of humidity; 19°C [day] to 15°C [night]) and then under long-day conditions (18 h cool white fluorescent light; 10,000 to 20,000 lux luminosity; 60 to 66% of humidity; 20.5°C [day] to 15°C [night]).

The single mutant phenotypes of *crc-1* modifiers were determined by analyzing progeny from 15 to 20 non-*crc* plants in F2 families (derived from double mutants crossed to the wild type) as F3 families. The homozygous T-DNA–tagged mutants were isolated in F2 progeny by PCR testing using a combination of gene and T-DNA–specific primers. Each mutant was backcrossed three times to the wild type, and in F2 generations, only plants homozygous for *crc-1* and either *rbl-1* or *sqn-4* or *ult1-4* displayed the FM indeterminacy phenotype. *ult1-4* was tested for cosegregation of the phenotype with the T-DNA and found to be tagged.

Desired mutant combinations were identified among phenotypic categories in the F2 segregants generated by cross-fertilizing heterozygote mutants. Genotypes were confirmed by monitoring Mendelian ratios and by progeny testing. Whenever necessary, theoretical and observed averages were compared using the $\chi^2$ test.

### Mutagenesis and Transformation

*crc-1* seeds were mutagenized with 25 mM EMS for 12 h and phenotypic modifiers selected in the M2 (Eshed et al., 1999). The T-DNA tagging screen used the plasmid pOCA28-15-991 (Eshed et al., 1999). The modifiers were backcrossed three times to wild-type L*er*. All transgenic plants were generated by the infiltration method described by Bechtold and Pelletier (1998) with selection on soil for resistance to the herbicide BASTA (Bayer; 0.05% of the commercial solution) or on Murashige and Skoog plates due to resistance to the antibiotic hygromycin (20 μg/L).

### Mapping and Molecular Identification of the Modifier of *crc* Genes

*rbl-1* and *sqn-4* were mapped by crossing *crc-1 rbl-1* and *crc-1 sqn-4* (L*er*) to *crc-8* (Col-0, SALK 065.539). *crc-8* contains a T-DNA insertion in the 4th intron of the gene that is associated with a 14-bp deletion from nucleotide positions 820 to 833 (relative to the translational start codon). Using cleaved amplified polymorphic sequence (CAPS) and simple sequence length polymorphism (SSLP) markers (Konieczny and Ausubel, 1993; Bell and Ecker, 1994), we established that *rbl-1* was localized on the right arm of chromosome 3 flanked by markers AP3-linked and CIW19 and *sqn-4* was on the left arm of chromosome 2 flanked by markers CIW3 and THY1. For the fine mapping, we designed new SSLP or CAPS markers that spanned the region between the respective markers, using the Monsanto Arabidopsis polymorphism and L*er* sequence database (http://www.arabidopsis.org/Cereon) as a source for potential single-nucleotide polymorphisms and small insertions/deletions between L*er* sequence and Col-0 sequence. The primer sequences, restriction enzymes, and number of restriction sites in the Col-0/L*er* ecotypes for the SSLP and CAPS marker sequences generated across these intervals are available upon request.

To isolate the *ult1-4* associated gene, we took advantage of the enhancer trap vector pOCA28-15-991 that allows plasmid rescue of flanked DNA sequences (Eshed et al., 1999).

Sequencing was performed on an ABI PRISM 3100 genetic analyzer sequencer (Perkin-Elmer) according to the manufacturer's instructions. Computer-based sequence analysis was performed using VectorNTI Suite (Informax) and Sequencher 4.0 (Gene Codes) software. Multiple alignments were obtained using ClustalX and edited with SeqVu (The Garvan Institute of Medical Research, Australia).

### RT-PCR

Total RNA was isolated from various tissues using Trizol reagent (Invitrogen) and treated with RNase-free DNaseI (Ambion). The first-strand cDNA synthesis was performed on 0.6 μg of total RNA using

RevertAid M-MuLV reverse transcriptase (Fermentas) and an oligo(dT) primer (18-mer) according to the manufacturer's instructions. From 20 μL of RT product, 1 μL was used for each PCR reaction. The annealing temperature was 55°C for all primer pairs, and 25 cycles of PCR were performed for all genes. After amplification, RT-PCR products were separated on agarose gel and stained with ethidium bromide.

### In Situ Hybridization, Toluidine and GUS Staining, and GFP Transient Expression

Tissue preparation, for both in situ hybridization and toluidine staining, was as described by de Almeida-Engler et al. (2001). Tissue sections were 10 μm thick. Probes for in situ hybridization were transcribed using digoxigenin labeling mix. *WUS* and *AG* templates were generated as previously described (Bowman et al., 1991; Mayer et al., 1998). *RBL* probe was synthesized in vitro from the PCR fragment containing 5′ ends of *RBL*. Whenever possible, constructs for the promoter and gene fusions upstream of *GUS*, *GFP*, and *RFP* reporter genes were made using the Gateway system. cDNA and DNA sequences were cloned into pDON207 vector and then transferred into the appropriate destination vector using LR cloning enzyme. We used pMDC162, pMDC107, and pMDC83 destination vectors for the *Pro:GUS*, *gene-GFP*, and *Pro35S:cDNA-GFP* constructs, respectively (Curtis and Grossniklaus, 2003), and pGIINK-GK7B 35Ster destination vector for the *gene-mRFP* constructs (Rotman et al., 2005). We always used the full intergenic sequences as promoter regions, except for the *ProRBL:RBL-mRFP* construct, in which we used 1.3 kb upstream of the first Met. GUS activity was assayed according to McConnell and Barton (1998). *Prom35S:cDNA-GFP* construct were also assayed by transient expression in tobacco (*Nicotiana tabacum*) leaves. Leaves were infiltrated as described (Rathjen et al., 1999), with an exponential phase culture *Agrobacterium tumefaciens* strain C58C1, diluted to an $OD_{600}$ of 0.5 with infiltration medium (10 mm MES, pH 5.6, 10 mm $MgCl_2$, and 200 μm acetosyringone).

### Microscopy

Plants were observed with a Leica MZFLIII stereomicroscope coupled to a DC300F digital camera (Leica Microsystems). Images were processed with the FW4000 software (Leica). Fresh flowers were also observed on a Hitachi S-3000N variable pressure scanning electron microscope. In situ hybridization signals and toluidine-stained tissues were visualized using a Nikon epifluorescence microscope (Optiphot-2) coupled with an Axio-Cam MRc digital camera (Carl Zeiss). Images were processed with the AxioVision software (Zeiss). GFP expression was monitored from homozygote plants using the Leica LSM-510 confocal microscope. All figures were composed with Adobe Photoshop 7.0 (Adobe Systems), and certain flower images have been treated to remove unrelated background.

### Accession Numbers

Arabidopsis Genome Initiative locus identifiers are as follows: *AP3* (AT3g54340), *AG* (AT4g18960), *CRC* (AT1g69180), *PI* (AT5g20240), *RBL* (AT3g55510), *SQN* (AT2g15790), *SUP* (AT3g23130), and *ULT1* (AT4g28190).

### Supplemental Data

The following materials are available in the online version of this article.

**Supplemental Figure 1.** Phenotypes of *rbl*, *sqn*, and *ult1* Allelic Lines Crossed with *crc-1*.

**Supplemental Figure 2.** Phenotype of *rbl-3*.

**Supplemental Figure 3.** Alignment of the Translation Products of At3g55510 (*RBL*) and At2g18220.

**Supplemental Figure 4.** Genomic and RT- PCR on the *ult1-4* Allele.

**Supplemental Figure 5.** Yeast Two-Hybrid Analysis of Binary Interactions between RBL, SQN, ULT1, and CRC.

**Supplemental Table 1.** Complementation Tests.

**Supplemental Data Set 1.** Fasta File Corresponding to the Alignment in Figure 2B.

## ACKNOWLEDGMENTS

This work was supported by the Agence Nationale de la Recherche through Grant ANR-05-BLAN-0280-01. We thank Christian Dumas and Jan Traas for supporting this project. We also thank Trudi Higginson, François Parcy, Mike Frohlich, Pradeep Das, Cédric Finet, Charlie Scutt, and Stève de Bossoreille for constructive discussions. We thank Isabelle Anselme-Bertrand and Béatrice Burdin for their help during scanning electron microscopy imaging, Claire Lionnet for her help during confocal microscopy, Edwige Moyroud and Cyrille Py for their excellent technical help, and Mathieu Reymond for naming *RBL*. We acknowledge Elliot Meyerowitz and Thomas Laux for providing the *Arabidopsis* mutants, Toshiro Ito for the AG antiserum, and Frank Wellmer for access to primary data on transcriptome profiles of flower homeotic mutants. We also thank the anonymous reviewers for their comments.

Received May 31, 2007; revised March 26, 2008; accepted April 5, 2008; published April 25, 2008.

## REFERENCES

**Alvarez, J., and Smyth, D.R.** (1999). CRABS CLAW and SPATULA, two Arabidopsis genes that control carpel development in parallel with AGAMOUS. Development **126:** 2377–2386.

**Amsterdam, A., Nissen, R.M., Sun, Z., Swindell, E.C., Farrington, S., and Hopkins, N.** (2004). Identification of 315 genes essential for early zebrafish development. Proc. Natl. Acad. Sci. USA **101:** 12792–12797.

**Angenent, G.C., Stuurman, J., Snowden, K.C., and Koes, R.** (2005). Use of Petunia to unravel plant meristem functioning. Trends Plant Sci. **10:** 243–250.

**Baum, D.A., and Hileman, L.C.** (2006). A genetic model for the origin of flowers. In Flowering and Its Manipulation, C. Ainsworth, ed (Sheffield, UK: Blackwell Publishing), pp. 3–27.

**Bechtold, N., and Pelletier, G.** (1998). In planta Agrobacterium-mediated transformation of adult *Arabidopsis thaliana* plants by vacuum infiltration. Methods Mol. Biol. **82:** 259–266.

**Bell, C.J., and Ecker, J.R.** (1994). Assignment of 30 microsatellite loci to the linkage map of Arabidopsis. Genomics **19:** 137–144.

**Berardini, T.Z., Bollman, K., Sun, H., and Poethig, R.S.** (2001). Regulation of vegetative phase change in *Arabidopsis thaliana* by cyclophilin 40. Science **291:** 2405–2407.

**Blazquez, M.A., Ferrandiz, C., Madueno, F., and Parcy, F.** (2006). How floral meristems are built. Plant Mol. Biol. **60:** 855–870.

**Bossinger, G., and Smyth, D.R.** (1996). Initiation patterns of flower and floral organ development in *Arabidopsis thaliana.* Development **122:** 1093–1102.

**Bowman, J.L., Drews, G.N., and Meyerowitz, E.M.** (1991). Expression of the Arabidopsis floral homeotic gene AGAMOUS is restricted to specific cell types late in flower development. Plant Cell **3:** 749–758.

**Bowman, J.L., Eshed, Y., Baum, S., Emery, J.F., Floyd, S.K., Alvarez, J., Hawker, N.P., Lee, J.Y., Siegfried, K.R., Khodosh, R.,**

**Tatom-Jaurez, M., and Perea, J.V.** (2001). The story of CRABS CLAW (or How we learned to love the mutagen). Flowering Newsletter **31:** 3–11.

**Bowman, J.L., Sakai, H., Jack, T., Weigel, D., Mayer, U., and Meyerowitz, E.M.** (1992). SUPERMAN, a regulator of floral homeotic genes in Arabidopsis. Development **114:** 599–615.

**Bowman, J.L., and Smyth, D.R.** (1999). CRABS CLAW, a gene that regulates carpel and nectary development in Arabidopsis, encodes a novel protein with zinc finger and helix-loop-helix domains. Development **126:** 2387–2396.

**Bowman, J.L., Smyth, D.R., and Meyerowitz, E.M.** (1989). Genes directing flower development in Arabidopsis. Plant Cell **1:** 37–52.

**Brand, U., Fletcher, J.C., Hobe, M., Meyerowitz, E.M., and Simon, R.** (2000). Dependence of stem cell fate in Arabidopsis on a feedback loop regulated by CLV3 activity. Science **289:** 617–619.

**Busch, M.A., Bomblies, K., and Weigel, D.** (1999). Activation of a floral homeotic gene in Arabidopsis. Science **285:** 585–587.

**Carles, C.C., Choffnes-Inada, D., Reville, K., Lertpiriyapong, K., and Fletcher, J.C.** (2005). ULTRAPETALA1 encodes a SAND domain putative transcriptional regulator that controls shoot and floral meristem activity in Arabidopsis. Development **132:** 897–911.

**Carles, C.C., and Fletcher, J.C.** (2003). Shoot apical meristem maintenance: The art of a dynamic balance. Trends Plant Sci. **8:** 394–401.

**Chen, X.** (2004). A microRNA as a translational repressor of APETALA2 in Arabidopsis flower development. Science **303:** 2022–2025.

**Chiurugwi, T., Pouteau, S., Nicholls, D., Tooke, F., Ordidge, M., and Battey, N.** (2007). Floral meristem indeterminacy depends on flower position and is facilitated by acarpellate gynoecium development in *Impatiens balsamina.* New Phytol. **173:** 79–90.

**Chuang, C.F., and Meyerowitz, E.M.** (2000). Specific and heritable genetic interference by double-stranded RNA in *Arabidopsis thaliana.* Proc. Natl. Acad. Sci. USA **97:** 4985–4990.

**Clark, S.E., Running, M.P., and Meyerowitz, E.M.** (1993). CLAVATA1, a regulator of meristem and flower development in Arabidopsis. Development **119:** 397–418.

**Clark, S.E., Running, M.P., and Meyerowitz, E.M.** (1995). CLAVATA3 is a specific regulator of shoot and floral meristem development affecting the same processes as CLAVATA1. Development **121:** 2057–2067.

**Curtis, M.D., and Grossniklaus, U.** (2003). A gateway cloning vector set for high-throughput functional analysis of genes in planta. Plant Physiol. **133:** 462–469.

**de Almeida Engler, J., De Groodt, R., Van Montagu, M., and Engler, G.** (2001). In situ hybridization to mRNA of Arabidopsis tissue sections. Methods **23:** 325–334.

**Dievart, A., Dalal, M., Tax, F.E., Lacey, A.D., Huttly, A., Li, J., and Clark, S.E.** (2003). CLAVATA1 dominant-negative alleles reveal functional overlap between multiple receptor kinases that regulate meristem and organ development. Plant Cell **15:** 1198–1211.

**Doerner, P.** (2006). Plant meristems: What you see is what you get? Curr. Biol. **16:** R56–R58.

**Endress, P.K., and Doyle, J.A.** (2007). Floral phyllotaxis in basal angiosperms: Development and evolution. Curr. Opin. Plant Biol. **10:** 52–57.

**Eshed, Y., Baum, S.F., and Bowman, J.L.** (1999). Distinct mechanisms promote polarity establishment in carpels of Arabidopsis. Cell **99:** 199–209.

**Ferrario, S., Immink, R.G., and Angenent, G.C.** (2004). Conservation and diversity in flower land. Curr. Opin. Plant Biol. **7:** 84–91.

**Fletcher, J.C.** (2001). The ULTRAPETALA gene controls shoot and floral meristem size in Arabidopsis. Development **128:** 1323–1333.

**Fletcher, J.C., Brand, U., Running, M.P., Simon, R., and Meyerowitz, E.M.** (1999). Signaling of cell fate decisions by CLAVATA3 in Arabidopsis shoot meristems. Science **283:** 1911–1914.

**Frohlich, M.W.** (2002). The mostly male theory of flower origins: Summary and update regarding the Jurassic pteridosperm Pteroma. In Developmental Genetics and Plant Evolution, Q.C. Cronk, R.M. Bateman, and J.A. Hawkins, eds (London: Taylor and Francis), pp. 85–108.

**Frohlich, M.W.** (2006). Recommendations and goals for evo-devo research: Scenarios, genetic constraint, and developmental homeostasis. Aliso **22:** 172–187.

**Gaiser, J.C., Robinson-Beers, K., and Gasser, C.S.** (1995). The Arabidopsis SUPERMAN gene mediates asymmetric growth of the outer integument of ovules. Plant Cell **7:** 333–345.

**Gibson, T.J., Ramu, C., Gemund, C., and Aasland, R.** (1998). The APECED polyglandular autoimmune syndrome protein, AIRE-1, contains the SAND domain and is probably a transcription factor. Trends Biochem. Sci. **23:** 242–244.

**Gomez-Mena, C., de Folter, S., Costa, M.M., Angenent, G.C., and Sablowski, R.** (2005). Transcriptional program controlled by the floral homeotic gene AGAMOUS during early organogenesis. Development **132:** 429–438.

**Hill, J.P., and Lord, E.M.** (1989). Floral development in *Arabidopsis thaliana*: A comparison of the wild-type and the homeotic *pistillata* mutant. Can. J. Bot. **67:** 2922–2936.

**Hublitz, P., et al.** (2005). NIR is a novel INHAT repressor that modulates the transcriptional activity of p53. Genes Dev. **19:** 2912–2924.

**Ito, T., Takahashi, N., Shimura, Y., and Okada, K.** (1997). A serine/threonine protein kinase gene isolated by an in vivo binding procedure using the Arabidopsis floral homeotic gene product, AGAMOUS. Plant Cell Physiol. **38:** 248–258.

**Jack, T.** (2004). Molecular and genetic mechanisms of floral control. Plant Cell **16** (suppl.): S1–S17.

**Jack, T., Sieburth, L., and Meyerowitz, E.** (1997). Targeted misexpression of AGAMOUS in whorl 2 of Arabidopsis flowers. Plant J. **11:** 825–839.

**Kamath, R.S., et al.** (2003). Systematic functional analysis of the *Caenorhabditis elegans* genome using RNAi. Nature **421:** 231–237.

**Konieczny, A., and Ausubel, F.M.** (1993). A procedure for mapping Arabidopsis mutations using co-dominant ecotype-specific PCR-based markers. Plant J. **4:** 403–410.

**Krizek, B.A., and Meyerowitz, E.M.** (1996). The Arabidopsis homeotic genes APETALA3 and PISTILLATA are sufficient to provide the B class organ identity function. Development **122:** 11–22.

**Laux, T., Mayer, K.F., Berger, J., and Jurgens, G.** (1996). The WUSCHEL gene is required for shoot and floral meristem integrity in Arabidopsis. Development **122:** 87–96.

**Lee, J.Y., Baum, S.F., Alvarez, J., Patel, A., Chitwood, D.H., and Bowman, J.L.** (2005). Activation of CRABS CLAW in the nectaries and carpels of Arabidopsis. Plant Cell **17:** 25–36.

**Lenhard, M., Bohnert, A., Jurgens, G., and Laux, T.** (2001). Termination of stem cell maintenance in Arabidopsis floral meristems by interactions between WUSCHEL and AGAMOUS. Cell **105:** 805–814.

**Lohmann, J.U., Hong, R.L., Hobe, M., Busch, M.A., Parcy, F., Simon, R., and Weigel, D.** (2001). A molecular link between stem cell regulation and floral patterning in Arabidopsis. Cell **105:** 793–803.

**Mayer, K.F., Schoof, H., Haecker, A., Lenhard, M., Jurgens, G., and Laux, T.** (1998). Role of WUSCHEL in regulating stem cell fate in the Arabidopsis shoot meristem. Cell **95:** 805–815.

**McConnell, J.R., and Barton, M.K.** (1998). Leaf polarity and meristem formation in Arabidopsis. Development **125:** 2935–2942.

**Milkereit, P., Gadal, O., Podtelejnikov, A., Trumtel, S., Gas, N., Petfalski, E., Tollervey, D., Mann, M., Hurt, E., and Tschochner, H.** (2001). Maturation and intranuclear transport of pre-ribosomes requires Noc proteins. Cell **105:** 499–509.

**Mizukami, Y., and Ma, H.** (1995). Separation of AG function in floral meristem determinacy from that in reproductive organ identity by expressing antisense AG RNA. Plant Mol. Biol. **28:** 767–784.

**Parcy, F., Nilsson, O., Busch, M.A., Lee, I., and Weigel, D.** (1998). A genetic framework for floral patterning. Nature **395:** 561–566.

**Rathjen, J.P., Chang, J.H., Staskawicz, B.J., and Michelmore, R.W.** (1999). Constitutively active Pto induces a Prf-dependent hypersensitive response in the absence of avrPto. EMBO J. **18:** 3232–3240.

**Ronse de Craene, L.P.** (2004). Floral development of *Berberidopsis corallina*: A crucial link in the evolution of flowers in the core Eudicots. Ann. Bot. (Lond.) **94:** 741–751.

**Rotman, N., Durbarry, A., Wardle, A., Yang, W.C., Chaboud, A., Faure, J.E., Berger, F., and Twell, D.** (2005). A novel class of MYB factors controls sperm-cell formation in plants. Curr. Biol. **15:** 244–248.

**Sablowski, R.** (2007). Flowering and determinacy in Arabidopsis. J. Exp. Bot. **58:** 899–907.

**Sakai, H., Krizek, B.A., Jacobsen, S.E., and Meyerowitz, E.M.** (2000). Regulation of SUP expression identifies multiple regulators involved in Arabidopsis floral meristem development. Plant Cell **12:** 1607–1618.

**Sakai, H., Medrano, L.J., and Meyerowitz, E.M.** (1995). Role of SUPERMAN in maintaining Arabidopsis floral whorl boundaries. Nature **378:** 199–203.

**Schoof, H., Lenhard, M., Haecker, A., Mayer, K.F., Jurgens, G., and Laux, T.** (2000). The stem cell population of Arabidopsis shoot meristems is maintained by a regulatory loop between the CLAVATA and WUSCHEL genes. Cell **100:** 635–644.

**Schultz, E.A., Pickett, F.B., and Haughn, G.W.** (1991). The FLO10 gene product regulates the expression domain of homeotic genes AP3 and PI in Arabidopsis flowers. Plant Cell **3:** 1221–1237.

**Shannon, S., and Meeks-Wagner, D.R.** (1993). Genetic interactions that regulate inflorescence development in Arabidopsis. Plant Cell **5:** 639–655.

**Sieburth, L.E., Drews, G.N., and Meyerowitz, E.M.** (1998). Non-autonomy of AGAMOUS function in flower development: use of a Cre/loxP method for mosaic analysis in Arabidopsis. Development **125:** 4303–4312.

**Sieburth, L.E., Running, M.P., and Meyerowitz, E.M.** (1995). Genetic separation of third and fourth whorl functions of AGAMOUS. Plant Cell **7:** 1249–1258.

**Smyth, D.R., Bowman, J.L., and Meyerowitz, E.M.** (1990). Early flower development in Arabidopsis. Plant Cell **2:** 755–767.

**Sommer, H., Beltran, J.P., Huijser, P., Pape, H., Lonnig, W.E., Saedler, H., and Schwarz-Sommer, Z.** (1990). Deficiens, a homeotic gene involved in the control of flower morphogenesis in *Antirrhinum majus*: The protein shows homology to transcription factors. EMBO J. **9:** 605–613.

**Szecsi, J., Joly, C., Bordji, K., Varaud, E., Cock, J.M., Dumas, C., and Bendahmane, M.** (2006). BIGPETALp, a bHLH transcription factor is involved in the control of Arabidopsis petal size. EMBO J. **25:** 3912–3920.

**Theissen, G., Becker, A., Winter, K.U., Munster, T., Kirchner, C., and Saedler, H.** (2002). How the land plants learned their floral ABCs: The role of MADS-box genes in the evolutionary origin of flowers. In Developmental Genetics and Plant Evolution, Q.C.B. Cronk, R.M. Bateman, and J.A. Hawkins, eds (London: Taylor and Francis), pp. 173–205.

**Trobner, W., Ramirez, L., Motte, P., Hue, I., Huijser, P., Lonnig, W.E., Saedler, H., Sommer, H., and Schwarz-Sommer, Z.** (1992). GLOBOSA: A homeotic gene which interacts with DEFICIENS in the control of Antirrhinum floral organogenesis. EMBO J. **11:** 4693–4704.

**Wellmer, F., Riechmann, J.L., Alves-Ferreira, M., and Meyerowitz, E.M.** (2004). Genome-wide analysis of spatial gene expression in Arabidopsis flowers. Plant Cell **16:** 1314–1326.

**Yanofsky, M.F., Ma, H., Bowman, J.L., Drews, G.N., Feldmann, K.A., and Meyerowitz, E.M.** (1990). The protein encoded by the Arabidopsis homeotic gene agamous resembles transcription factors. Nature **346:** 35–39.

**Zhao, L., Kim, Y., Dinh, T.T., and Chen, X.** (2007). miR172 regulates stem cell fate and defines the inner boundary of APETALA3 and PISTILLATA expression domain in Arabidopsis floral meristems. Plant J. **51:** 840–849.